# Chapter 7: Molecular Dual Fluorescent Materials

## Synthesis and Studies on Dual fluorescent 4-Thiocyanato aniline and its derivatives

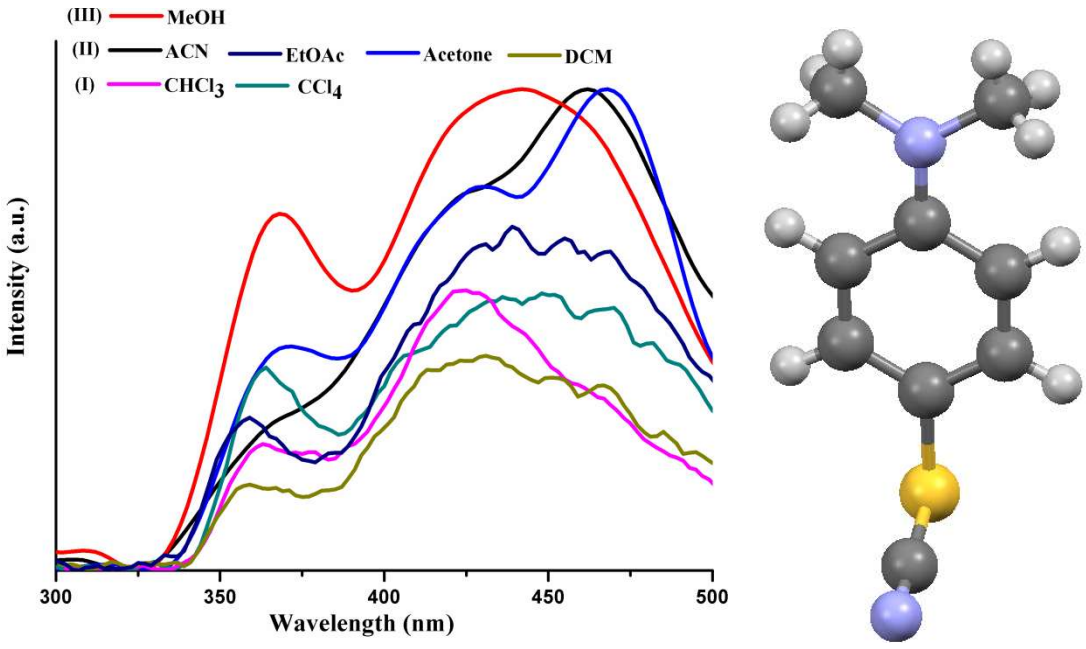

Excitation of molecules by light if results in absorption and then subsequent emission with higher wavelength (over energy) is known as fluorescence, a well known radiative photo-physical phenomena, as shown in Figure 7.1. In fluorescence, a fluorophore absorbs light energy and populates higher vibrational energy before getting rapidly relaxed to the lowest excited electronic state ($\mathbf{S_1}$), in the form of **vibrational relaxation** or **internal conversion**. Therefore, Fluorescence usually originates from $\mathbf{S_1}$ irrespective of the excitation wavelength and hence, the fluorescence spectrum of a molecule is characterized by a signal band. The electronic transitions are instantaneous in nature, occurring in short timeframes (nano to sub-pico seconds).

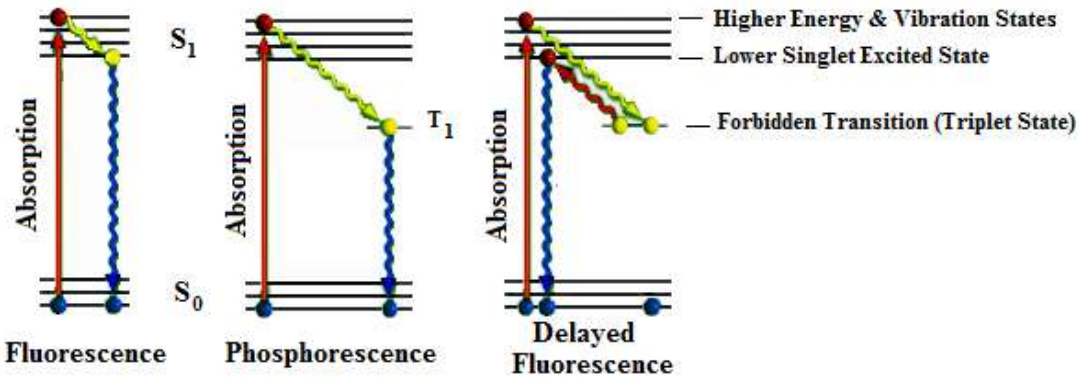


**Fig. 7.1: Jablonski diagram illustrates a *singlet* ground electronic state (the parallel bars labeled S(0)), as well as *singlet* first (S(1); upper set of parallel bars, sphere representing an electron)**

Other prominent radiative photo-physical phenomenon is phosphorescence. In phosphorescence, electron undergoes a spin conversion into a "forbidden" triplet state ($\mathbf{T_1}$) instead of the lowest singlet excited state, a process known as intersystem crossing before returning to the ground state. Emission from $\mathbf{T_1}$ state occurs with lower energy relative to fluorescence and emitted photons have much longer wavelengths.

*4-(N,N-dimethylamino)-benzonitrile (DMABN) a very special molecule, Why?*

DMABN is of the smallest molecules with strong electron donor and electron acceptor in conjugation. This is one of the origins for exhibiting anomalous emission properties such as large Stokes shifts and/or dual-luminescence. A latter phenomenon was observed by Lippart, and described two emissions as $\boldsymbol{F_A}$ (A-fluorescence) and $\boldsymbol{F_B}$ band (B-fluorescence) [1].

Many mechanisms were proposed for the observed dual fluorescence of DMABN. One early one is, 'state Reversal' or $F_B \rightarrow F_A$ inversion' model as shown in Figure 7.2a. According to this simple model, DMABN has two close –laying exited states, indicated here as A and B states. Figure 7.2b shows the fluorescence spectrum of DMABN with two emission bands, a shorter wavelength one is described as 'anomalous' or $F_A$ band. Here, dual emission can be correlated to internal charge transfer processes (ICT) between adjacent electron donor and electron acceptor groups in the emitting excited state.

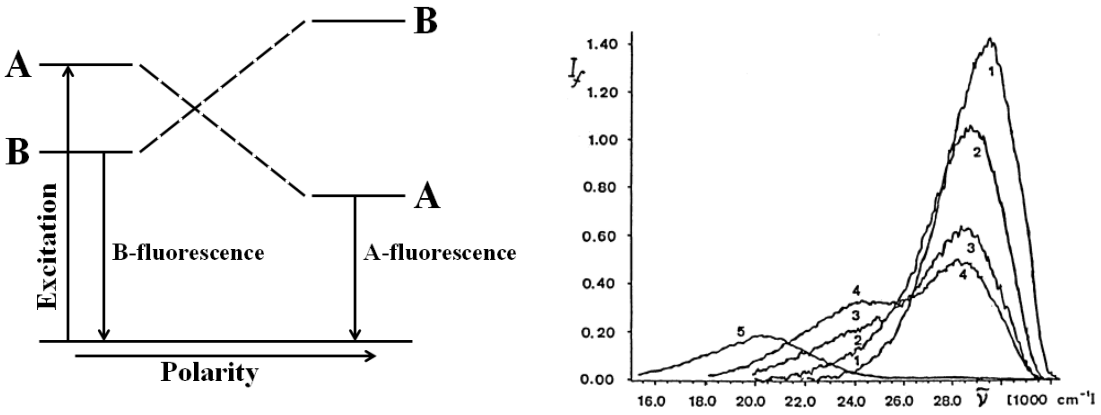


(a) (b)

**Fig. 7.2: (a) Pictorial presentation of State reversal model (b) Fluorescence spectra of DMABN (1) in several solvents: (1) n-hexane, (2) dibutyl ether, (3) diethyl ether, (4) butyl chloride, and (5) acetonitrile [2]**

Interestingly, ICT process perturbs the atomic charge distribution of the molecule and changes the dipole moment, which is greater in excited states compared to the ground state. This results in the solvent polarity driven $F_A$ fluorescence. An increased in the polarity of the medium leads to drastic shift of maxima towards the longer wavelength. That means excited state is very sensitive to the environment when the molecule is dissolved in polar solvent. In non polar media, the less polar 'B- state ($F_B$)' is the lowest excited state from which the florescence originates. However, in polar media, stabilization of the highly polar 'A- state' brings it below the 'B-state' making it the lowest state.

Different types of mechanisms were proposed to explain dual fluorescence of DMABN. These are listed below,

- an excimer formation [3],
- a protonated species formation [4],
- an exciplex formation with solvent [5],
- an intramolecular structural change by a 90° twist of the amino group (TICT) [6],
- a *pseudo-Jahn-Teller* (PJT) distortion or a rehybridization (pyramidalization, inversion, wagging) of the amino group (WICT) [7],
- a rehybridisation (bending) of the cyano group (RICT) [8] and by the planarization of the molecule in the CT state (PICT) [9].

Most debated mechanism is based on a twisted intramolecular Charge transfer (TICT), as shown in Figure 7.3.

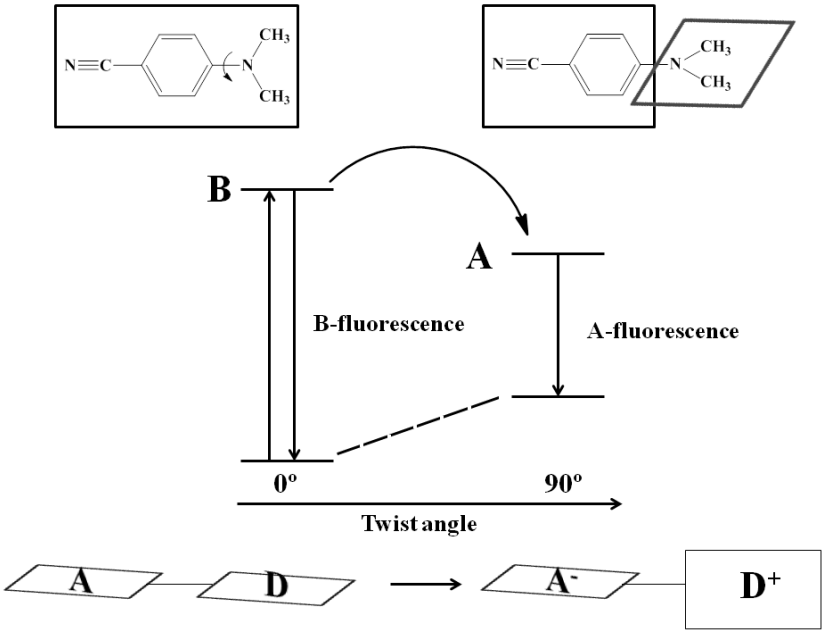


**Fig. 7.3: The twisted intramolecular Charge transfer (TICT) model**

According to this mechanism, $F_B$ fluorescence arises from a coplanar stricter of DMABN, whereas $F_A$ fluorescence originates from a stricter in which the dimethyl amino (-$NMe_2$) group is twisted 90º with respect to the cyano phenyl moiety. The high dipole moment associated with the stricter is attributed to the transfer of one electron

from electron rich donor -$NMe_2$ group (D) to the electronically deficient cyano phenyl accepter (A) group. A quantitative study using different solvents showed change in dipole moment in DMABN molecule in the ground and excited state is of the order of 23 D. For general reference, dipole moment of benzonitrile molecule is 4.3D [10]. The state reversal model does not involve any change in the molecule structure, whereas the concept of structural change is key to the TICT Mechanism, as shown in Figure 7.2.

**Motivation**: Rotation of an electron donor (ED) group or wagging of electron acceptor (EA) group played an important role in observing dual fluorescence in molecular compounds. Is it possible to design rotating EA group? Will it affect dual florescence?

**Probable solution:** Use of strong and slightly long electron acceptor group and sterically hindered electron donating group.

**Abstract:**

**Part I** of this chapter will cover synthesis of four new 4-thiocyanato substituted aniline compounds, from aniline and its derivatives as shown below with a general formula 4-SCNAn, [where, An = aniline (**1**), N-methyl aniline (**2**), N, N-dimethyl aniline (**3**) and 2,6-dimethyl aniline (**4**)]. All the synthesized compounds were characterized by elemental analysis, FT-IR and NMR spectroscopy. Three compounds, **1**, **2** and **4**, are crystallized in monoclinic crystal system. Compound **1** has space group $P2_1/n$ with cell dimensions a = 12.3604(7)Å, b = 4.42635(18)Å, c = 13.4575(6)Å, V = 733.70(6)Å$^3$ and Z = 4; compound **3** has space group $P2_1/m$ with cell dimensions a = 4.4592(2)Å, b = 9.9631(4)Å, c = 10.2383(5)Å, V = 454.74(4)Å$^3$ and Z = 2 while compound **4** has space group $P2_1/c$ with cell dimensions a = 11.529(2) Å, b = 4.2355(8) Å, c = 19.235(3) Å, V = 899.9(3) Å$^3$ and Z = 4. All the compounds showed dual fluorescence may be due to rotation of –SCN moiety and/or due to twisting of amino group in excited state. All compounds **1-4** showed different fluorescence behavior in polar and non polar solvents. The intensity of $\boldsymbol{F_A}$ and $\boldsymbol{F_B}$ band depend on the polarity of solvent and substituent on the amino group.

In **Part-II**, salt formation of 4-thiocyanato aniline (**1**), studied inpart I, was planned to understand the effect of thiocyanato moiety alone on dual fluorescence. We have synthesized two new thiocyanato substituted aniline salts ($HNO_3$-**5,** HCl-**6**) from compound **1**. Both the compounds crystallized in monoclinic crystal system. Compound **5** crystallized in space group $P2_1/c$ with cell dimensions : a = 5.7550(1)Å, b = 8.0389(1)Å, c = 19.6350(4)Å, V = 908.27(3) Å$^3$ and Z = 4. While compound **6** crystallized in space group $P2(1)/n$ with cell dimensions a = 5.6625(1)Å, b = 17.6032(4)Å, c = 8.2897(2)Å, V = 825.62(3)Å$^3$ and Z = 4. Single crystal X-ray study has shown that after salt formation thiocyanato moiety became planar with phenyl ring. Thus changes in geometry around electron acceptor group and protonation of electron donor group resulted in quenching of dual fluorescence of these compounds.

Thus, this set of compounds is in-directly confirming role of 'motion' of thiocyanato group for dual fluorescence.

**Part-I: Study of thiocyanato aniline**

## 7.1 Introduction

**Comparison between DMABN and Compounds in present investigation:**

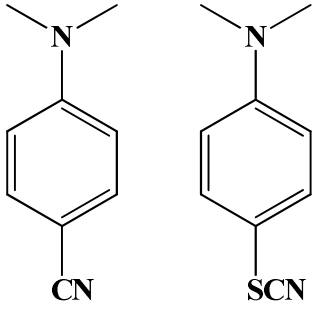


**DMABN** **DMATCB (3)**

**Scheme 7.1: Structure of dimethyl amino benzonitrile (DMABN) and dimethyl amino thiocyanato benzene-3 (DMATCB)**

Dual fluorescence of DMABN strongly depended on solvent polarity and temperature. In nonpolar solvents, only one fluorescence band appears, originating from the $^1L_b$ ($^1B_2$) state knows as B fluorescence ($\boldsymbol{F_B}$), or normal fluorescence (**FN**), or locally excited fluorescence (**LE**) [11]. In polar solvents, a further long-wavelength fluorescence band grows in relative intensity, while the intensity of the first band decreases with the increasing polarity of the medium. Solvent polarity exerts its influence in the form of a strong solvatochromic shift of the $\boldsymbol{F_A}$ band (Figure 7.1b) and an increasing ratio of intensities, $\boldsymbol{F_A/F_B}$. According to TICT model, much discussed model, DMABN showing $\boldsymbol{F_B}$ band is assigned to an approximately coplanar structure and $\boldsymbol{F_A}$ to a CT excited-state conformation with a highly twisted $NMe_2$ group, possibly perpendicular to the aromatic ring.

**DMATCB** (dimethyl amino thiocyanato benzene) is similar to DMABN; with difference lies in the electron acceptor group. In **DMATCB** thiocyanato group instead of cyano group is employed as an electron acceptor. Sulphur atom is well known to pull electron density away from aromatic ring [12]. Therefore, two additional features of thiocyanato (-SCN) moiety are (i) it can rotate freely so as stabilize polar state (or destabilize coplanar state), and (ii) it can be polarized through pair of electrons residing on S- atom.

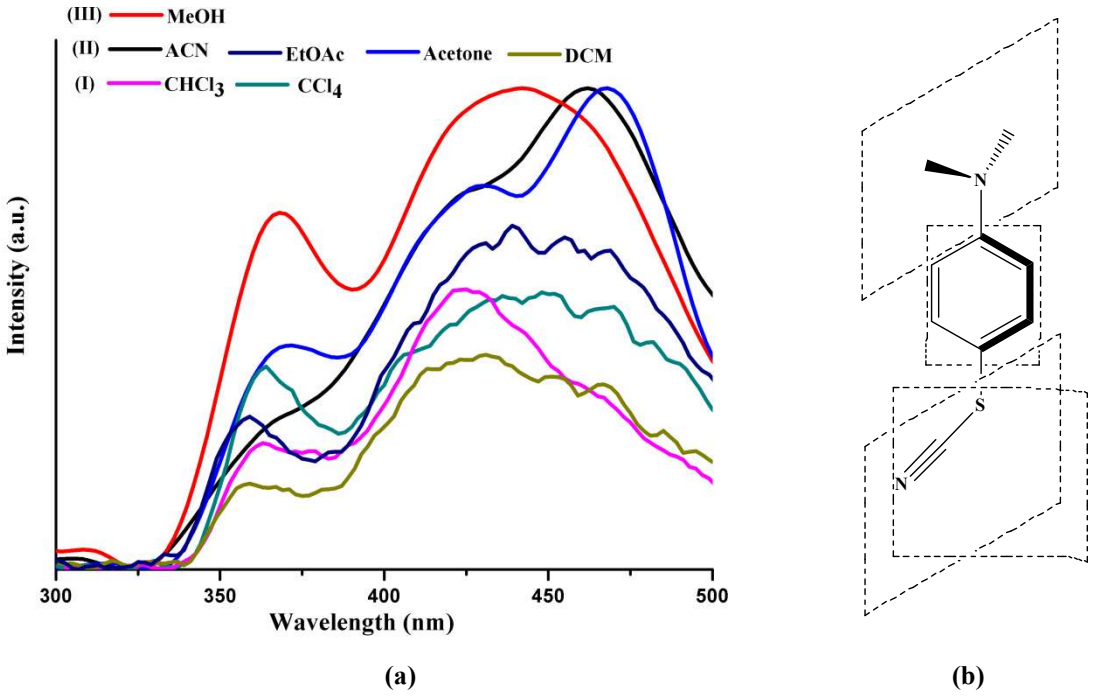


(a) (b)

**Fig. 7.4: (a) Fluorescence spectra of DMABN (I) in non polar solvents: (1) chloroform, (2) $CCl_4$; (II) in polar aprotic solvents: (1) DCM, (2) ACN, (3) EtOAc, (4) Acetone; (III) in polar protic solvent: (1) Methanol. (b) Possible twisting or rotation of Donor as well as Acceptor group**

As per expectations, **DMATCB** (**3**) also showed dual fluorescence. Contrary to DMABN; in nonpolar solvents as well compound-**3** showed dual fluorescence as shown in Figure 7.4a(I). It indicates the low-lying, strongly polar excited state of **3**, with bent SCN group is possible $\boldsymbol{F}_{\mathbf{A}}$ emitter. This result finds similarity with carbonyl substituted aniline derivatives in literature [13]. In polar aprotic solvents (Figure 7.4a-II), the intensity of long-wavelength fluorescence band $\boldsymbol{F}_{\mathbf{A}}$ grows, while the intensity of the first band decreases indicates towards TICT mechanism. Along with it one more band is observed, i.e. $\boldsymbol{F}_{\mathbf{A2}}$ must be attributed to the main absorption band of the monomeric molecules, and it seems to originate from a TICT state. In polar solvent, methanol, both bands ($\boldsymbol{F}_{A}$ and $\boldsymbol{F}_{B}$) were observed but with absence of $\boldsymbol{F}_{\mathbf{A2}}$ band. Apart from emission in chloroform and DCM, $\boldsymbol{F}_{\mathbf{A}}$ band shift to red shift in all solvents. Thus, in present set compounds both group's, electron donor and electron-acceptor, i.e. dimethyl amino and SCN group, can rotate or twist made to us to extend TICT hypothesis in the form of Figure 7.4(b).

Similar observation was observed to support this hypothesis comes from geometry optimization of the ground state along the-$NH_2$ wagging and -$NO_2$ twisting coordinates revealed the fact that the -$NO_2$ group rotates freely in the ground-state and the charge-transfer absorption band is broadened because of distribution of -$NO_2$ conformers around the coplanar conformation of the benzene moiety [14]. However, in the excited electronic state, the -$NO_2$ group is oriented orthogonal to the benzene ring. Hence the internal conversion process was governed by the twisting of the Nitro group to the perpendicular conformation toward the deep minimum of the potential energy surface (PES) along the twisting coordinate.

Hence to check this hypothesis and understand possible twisting of amino (-$NMe_2$) moiety and rotation of -SCN effect on fluorescence spectra, a series of model compounds were synthesized by changing alkyl groups on amino functionality (**1, 2**), and/or adding sterically hindering substituent's (**4**).

## 7.2 Experimental

### 7.2.1 Materials and Methods:

All chemicals and solvents were of analytical grade reagents. Aniline, N-methyl aniline, N,N-dimethyl aniline and 2,6-dimethyl aniline were from s.d. fine chemicals; ammonium thiocyanato (Aldrich), iodine (Merck) and methyl alcohol (Qualigens) were used without further purification.

### 7.2.1 Syntheses of 4-thiocyanato aniline and derivatives:

A general methodology of 4-thiocyanato aniline preparation/syntheses is mentioned in scheme-7.2.

**Scheme: 7.2**

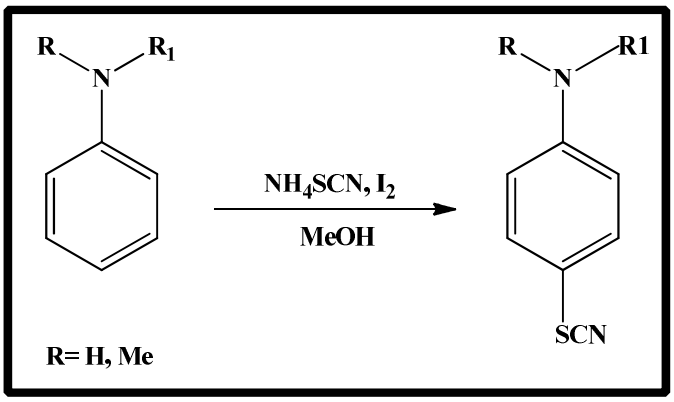


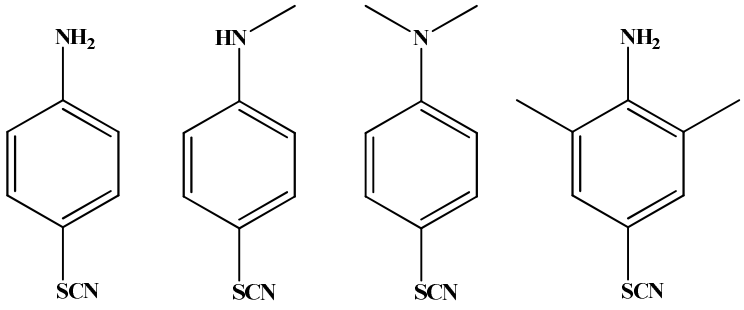


(1) (2) (3) (4)

**Scheme: 7.3 - Proposed reaction mechanism**

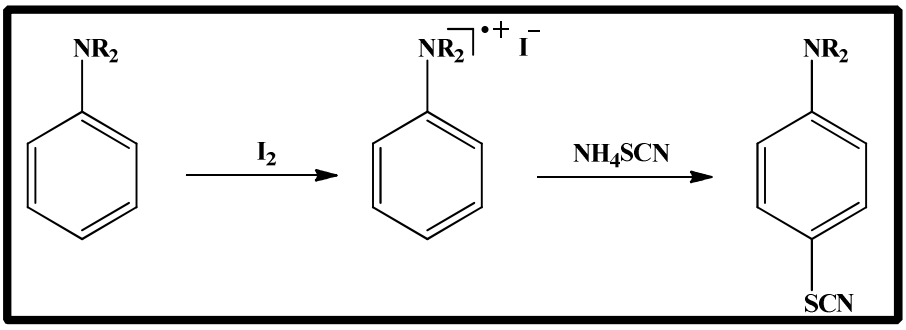


A methanolic solution (50 mL) containing ammonium thiocyanate (0.016 mol) and iodine (0.00547mol) were mixed and stirred for 15 min. The aryl amine (0.0054 mol) was added drop wise to this reaction mixture with continuous stirring. After completion of addition of aryl amine, reaction mixture stirred for 25 min. Progress of the reaction was monitored by TLC. After completion of reaction, 75 mL water was added to reaction mixture and reaction mixture stirred for 15 mins. The whole reaction mixture was transferred to 500 ml beaker and 75 mL dichloromethane was added to it. The two layers were formed; the layers were stirred vigorously for 10 min. The layers were transferred to separating funnel for separation. DCM layer separated from it. The remnant was again treated with fresh DCM and the whole process repeated. All DCM layers were combined and washed with 50 mL water (two times). The final separated DCM layer was treated with $Na_2SO_4$ for removal of water. The DCM layer was then concentrated on a rotary evaporator to obtain the thiocyanato compound, final product.

The compound was further purified by column chromatography using n-Hexane: Ethyl acetate solvent system.

Compound **2, 3** and **4** were obtained using a similar method to that of **1**, except that N-methyl aniline, N, N-dimethyl aniline and 2, 6-dimethyl aniline was used.

Colorless plate-shaped crystals of **1** suitable for X-ray diffraction were obtained by slow evaporation of the solvents within 1 day.

**Table 7.1: Percentage yield of Thiocyanato aniline and Derivative**

| Entry | Compound | % Yield | Colour |
|---|---|---|---|
| **1** | 4-thiocyanato aniline | 80 % | Pale Yellow |
| **2** | N- methyl-4- thiocyanato aniline | 64 % | Colorless |
| **3** | N,N- dimethyl-4- thiocyanato aniline | 72 % | Colorless |
| **4** | 2,6-dimethyl-4- thiocyanato aniline | 84 % | Colorless |

## 7.3 Result and Discussions

### 7.3.1 FT-IR:

FT-IR spectra for a series of 4-thiocyanato aniline were recorded in the range of 4,000 - 400 $cm^{-1}$ at RT.

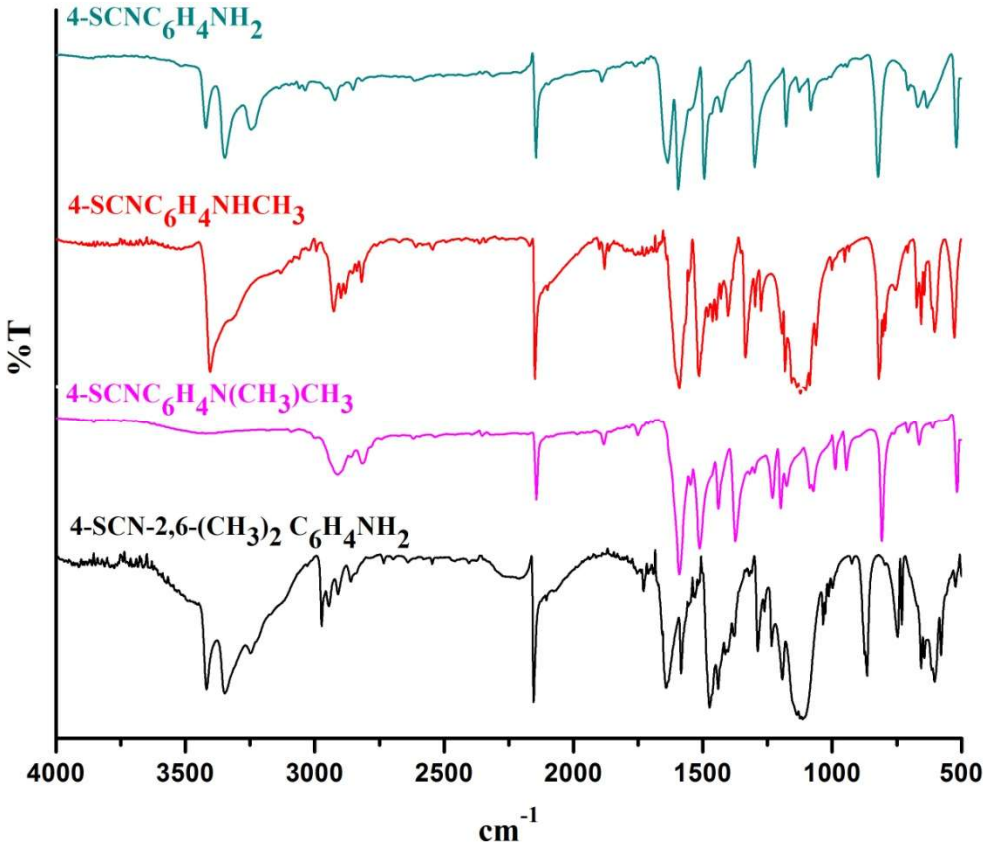


**Fig.7. 5: FT-IR of compounds 1, 2, 3 and 4**

**Compound 1 - FT-IR (KBr):** 3422 (vs), 3349(vs), 3246 (vs), 3137(w), 3099 (w), 3062 (w), 3035 (w), 2959(w), 2919 (m), 2890 (w), 2853 (m), 2818(w), 2145 (ssh), 2097 (w), 1890(s), 1758 (w), 1637 (vs), 1596 (vssh), 1543 (s), 1494 (vssh), 1465 (s), 1429 (s), 1350 (w), 1301 (vssh), 1179 (vs), 1127 (s), 1084 (s), 1022(w), 1002 (w), 956 (w), 943 (w), 894 (w), 821 (vssh), 707 (m), 671 (s), 631 (s) and 520 (vs) $cm^{-1}$.

**Compound 2- FT-IR (KBr):** 3405 (vs), 3310 (s), 3130(w), 2925 (s), 2901 (m), 2880(m), 2819 (m), 2609(w), 2544 (w), 2170 (w), 2146 (ssh), 2097 (w), 1901 (w), 1882 (m), 1593 (vs), 1563 (s), 1516 (vs), 1481 (w), 1461 (m), 1449 (m), 1429 (w), 1402 (s), 1335 (ssh), 1297 (m), 1276 (s), 1195 (m), 1183 (s), 1159 (s), 1138 (vs), 1123 (vs), 1103 (s), 1087 (s),

1063 (m), 1002 (m), 951 (m), 935 (w), 820 (vs), 805 (s), 793 (s), 756 (m), 709 (w), 674 (s), 656 (s), 645 (m), 617 (s), 604 (s), 527 (vs), 476 (s), 421 (m) and 410 (m) $cm^{-1}$.

**Compound 3- FT-IR (KBr):** 3089 (w), 2999 (w), 2909 (s), 2857 (m), 2814 (s), 2740(w), 2617 (w), 2593 w), 2531 (w), 2142 (ssh), 1885 (m), 1750 (m), 1592 (vssh), 1548 (m), 1515 (vs), 1463 (m), 1440 (s), 1374 (vs), 1320 (w), 1299 (w), 1230 (s), 1197 (vs), 1174 (s), 1128 (w), 1087 (s), 1072 (vs), 987 (s), 944 (s), 808 (vssh), 759 (w), 705 (m), 664 (m), 610 (m) and 520 (vs) $cm^{-1}$.

**Compound 4- FT-IR (KBr):** 3418 (vs), 3347 (vs), 3250 (s), 3168 (w), 3029 (w), 2975 (vs), 2944 (s), 2910 (s), 2858 (m), 2836 (m), 2734 (w), 2641 (w), 2545 (w), 2401 (w), 2152 (ssh), 2103 (m), 1728 (m), 1658 (w), 1641 (vs), 1585 (s), 1564 (w), 1556 (w), 1549 (w), 1537 (m), 1530 (m), 1519 (w), 1513 (w), 1474 (vs), 1462 (s), 1441 (s), 1428 (w), 1414 (m), 1402 (m), 1378 (m), 1321 (w), 1311(w), 1288 (vs), 1261 (m), 1235 (s), 1193 (s), 1137 (vs), 1124 (s), 1113 (s), 1035 (m), 1027 (m), 1013 (m), 999(m), 924(w), 875 (vs), 864 (vs), 798 (w), 748 (s), 731 (s), 700 (w), 674 (w), 657 (s), 644 (m), 615 (s), 603 (vs), 578 (s), 524 (m), 501 (m), 460 (m) and 439 $cm^{-1}$.

It is observed that $-NH_2$ symmetric and antisymmetric stretching observed in the range of 3418-3246 $cm^{-1}$ in compounds **1**, **2** and **4**. Compounds **2**, **3** and **4** showed aliphatic $-CH_3$ stretching band observed around in the range of 3168-2814 $cm^{-1}$ while $-CH_3$ symmetric deformation mode observed in the range of 1374-1311 $cm^{-1}$ and at 1288-1123 $cm^{-1}$. The bands in the region 3250-2600 $cm^{-1}$ contains the N-H stretching vibrations were observed due to the continuous series of overlapping bands, combination and overtone bands. Sharp-strong modes at 2152-2142 $cm^{-1}$ confirmed the cyano frequency for the SCN triple bond stretching vibration. Lower values for cyano frequency in SCN triple bond can be explained on the basis of reverse substituent effect on SCN moiety. Here it is the effect of the substituent X on the electron density and hence on the stretching frequency of the SCN triple bond as shown by the canonical forms (a) and (b) [15].

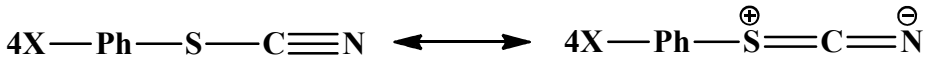


**(a)** **(b)**

**X= $-NH_2$, $NMe_2$, -NHMe**

Thus, an electron-donating substituent X will favour (b), with a CN bond order of two and hence a lower $\upsilon_{SCN}$. The bands also observed at 1179 - 1002 $cm^{-1}$ due to aliphatic C-N stretching and 1340 - 1250 $cm^{-1}$ due to primary aromatic C-N stretching in all compounds.

The C-H ring stretching modes were observed in the range of 1641-1429 $cm^{-1}$. *in- plane* CH deformation modes were observed in the range of 1215-1015 $cm^{-1}$ while out-of-plane deformation modes in the range of 864-631 $cm^{-1}$. Strong band observed at 865-807 $cm^{-1}$ were assigned to C-S bond. Sharp medium bands were observed at 756-705 $cm^{-1}$ assigned to the *out-of- plane* ring deformation.

### 7.3.2 Elemental analyses:

The calculated elemental analyses were consistent with the observed formulae of thiocyanato compounds.

**Compound 1:Anal. Calc. for** $C_7H_6N_2S$: C, 55.97; H, 4.03; N, 18.65; S, 21.35%; **Found:** C, 55.98; H, 3.99; N, 18.66; S, 21.35%.

**Compound 2:Anal. Calc. for** $C_8H_8N_2S$: C, 58.51; H, 4.91; N, 17.06; S, 19.52%; **Found:** C, 58.52; H, 4.87; N, 17.10; S, 19.51%.

**Compound 3:Anal. Calc. for** $C_9H_{10}N_2S$: C, 60.64;H, 5.65; N, 15.72; S, 17.99%; **Found:** C, 60.58; H, 5.61; N, 15.70; S, 17.96%.

**Compound 4:Anal. Calc. for** $C_9H_{10}N_2S$:C, 60.64; H, 5.65; N, 15.72; S, 17.99%; **Found:** C, 60.65; H, 5.61; N, 15.72; S, 17.97%.

### 7.3.2 $^1$H NMR Spectra:

A formation of 4-thiocyanato aniline and its derivatives has been confirmed by $^1$H NMR spectroscopy (Figure 7.6-7.9). The details of $^1$H NMR spectra for all these compounds are tabulated in Table 7.2

**Table 7.2: Details of $^1$H NMR spectra of compounds 1, 2, 3 and 4**

| Compounds | (δ value) $^1$H NMR (d6-DMSO) J coupling in Hz |
|---|---|
| (**1**) | δ 5.809 (s 2H, $NH_2$), 6.618-6.639 (q, 2H, J = 2.0 and 4.4), 7.318-7.331 (q, 2H, J = 1.6 and 5.2). |
| (**2**) | δ 4.236 (s 2H, $NH_2$), 6.603-6.625 (d 2H, J = 8.8), 7.399-7.421 (d 2H, J = 8.8), 2.872 (s 3H, $CH_3$). |
| (**3**) | δ 6.769-6.792 (dd 2H, J = 2.0 and 4.8), 7.458-7.480 (dd 2H, J = 2.4 and 4.8), 2.952 (s, 6H, $CH_3$). |
| (**4**) | δ 3.851 (s 2H, $NH_2$), 7.194(s 2H), 2.193(s, 6H, $CH_3$). |

.It is observed that in compound **1,** the N–H protons (**a**) are in high field (δ = 5.809 ppm), and aromatic protons appear at 6.618–7.331 ppm. The N-H protons consist of a singlet while aromatic region shows quartet for *ortho*-hydrogen's (δ = 6.618 to 6.639 ppm) and (δ = 7.310 to 7.331 ppm) for the *meta*-protons. Similar observation has been obtained for compound **2**. The N-$CH_3$ (methyl) showed the singlet at the high field region at δ = 2.952 ppm. Aromatic protons showed doublets appear on δ =6. 769- 6.692 ppm for *ortho*-hydrogen and δ =7.458-7.480 ppm for the *meta*-hydrogen. Compound **3** showed the N-$CH_3$ protons are in high field at δ = 2.952 ppm and peaks around δ = 6.769-6.792 ppm and δ = 7.458-7.480 ppm indicate the aromatic *ortho* and *meta* protons respectively. In case of compound **4**, –$CH_3$ protons are in high field region showed singlet at δ = 2.193 ppm while aromatic protons at δ = 7.194 ppm and N-H protons consist of a singlet at δ = 3.851 ppm.

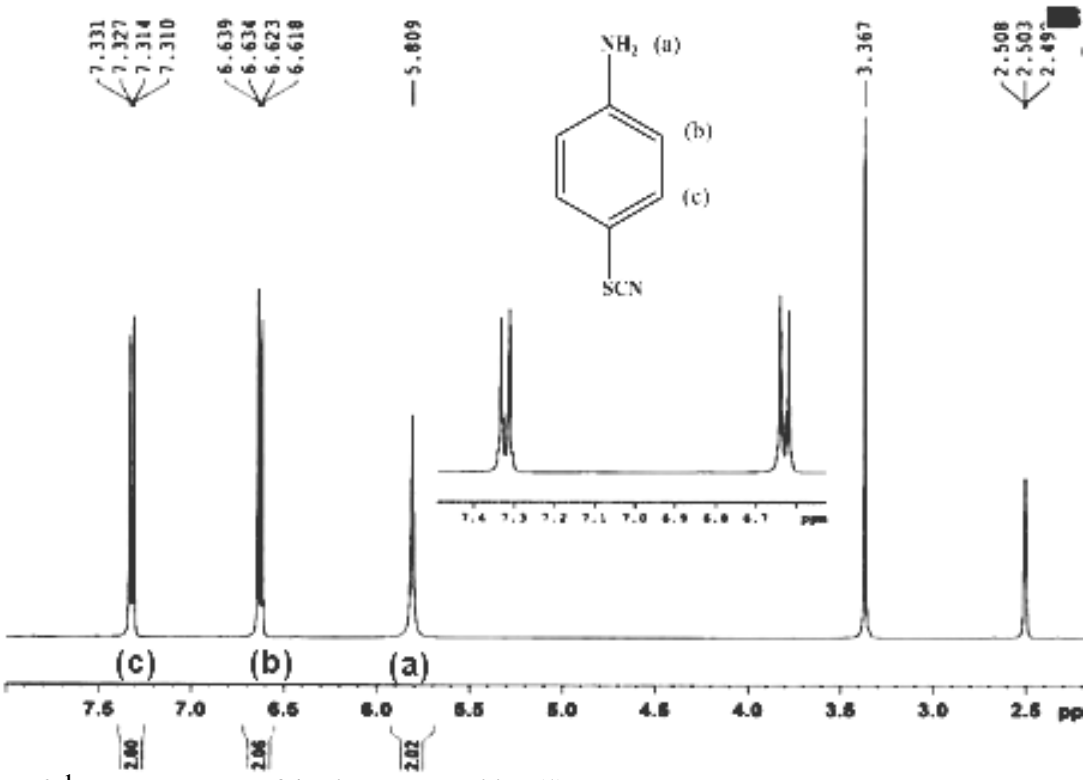


**Fig.7. 6: $^{1}$H NMR spectra of 4-thiocyanato aniline (1)**

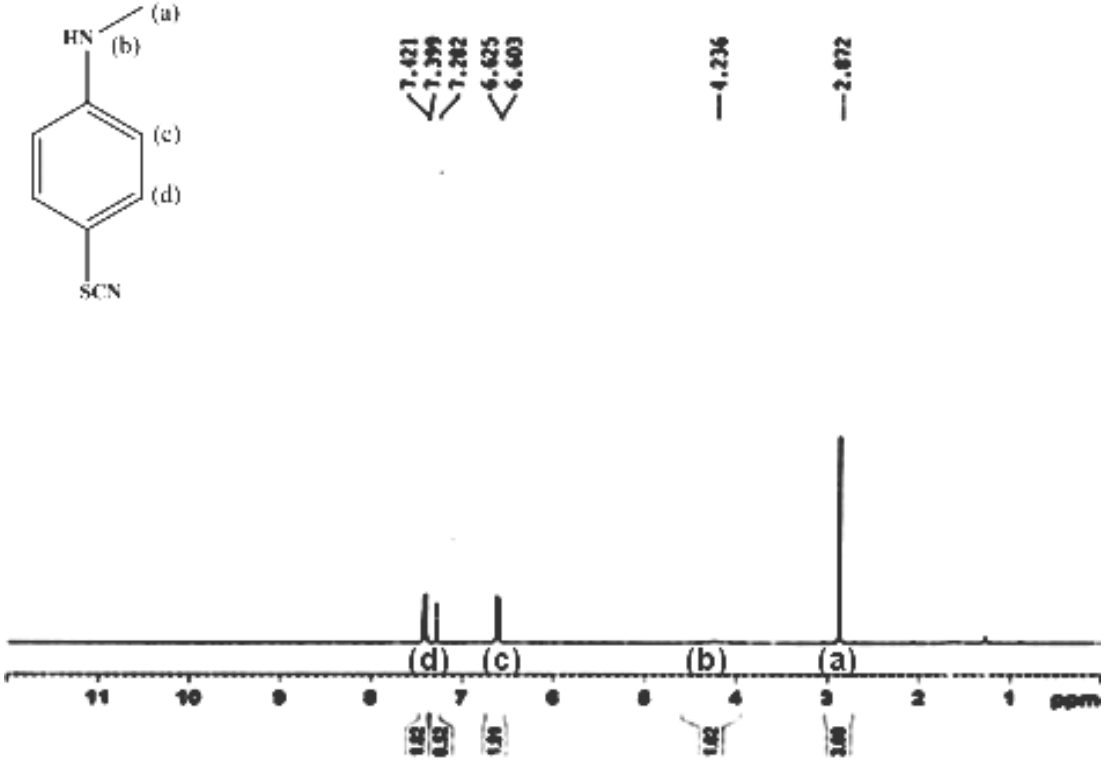


**Fig. 7.7: $^{1}$H NMR spectra of N- methyl-4-thiocyanato aniline (2)**

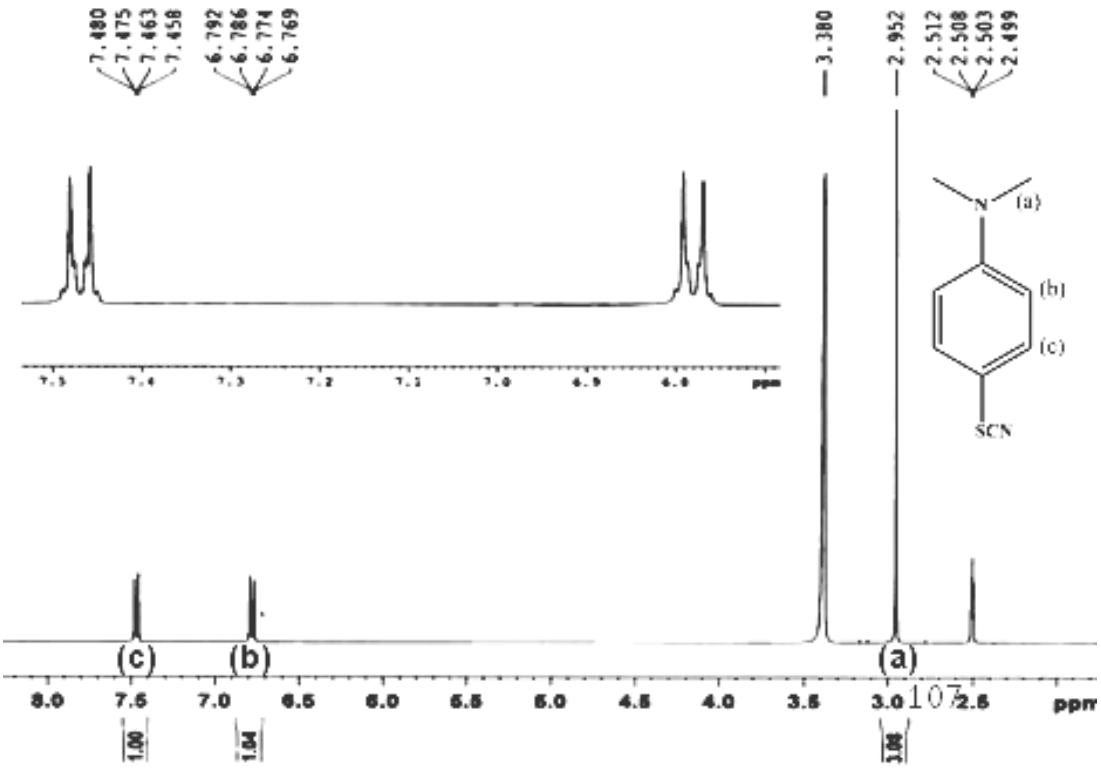


**Fig. 7.8: $^{1}$H NMR spectra of N, N- dimethyl-4-thiocyanato aniline (3)**

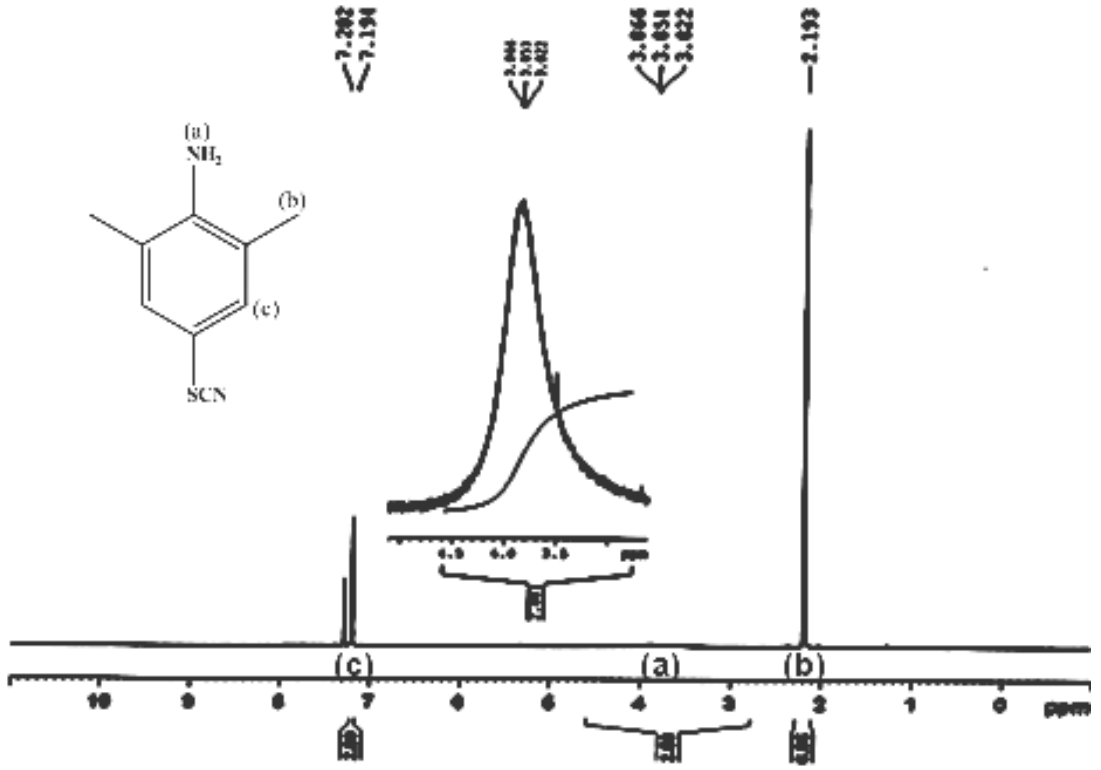


**Fig. 7.9: $^{1}$H NMR spectra of 2,6-di methyl-4-thiocyanato aniline (4)**

## 7.4 Thermal Studies

### 7.4.1 TG-DTA:

Thermo-gravimetric studies (TG/DTA) were carried out in nitrogen atmosphere in the 300-850 K temperature range on powdered samples. Figure 7.10 showed thermal analyses of compounds **1, 2, 3** and **4**. The two step decomposition patterns of **1**, **2** and **4** are quite similar and can be generalized by saying that decomposition steps are accompanied by the gradual loss of number of aniline moiety followed by mass loss of SCN moiety.

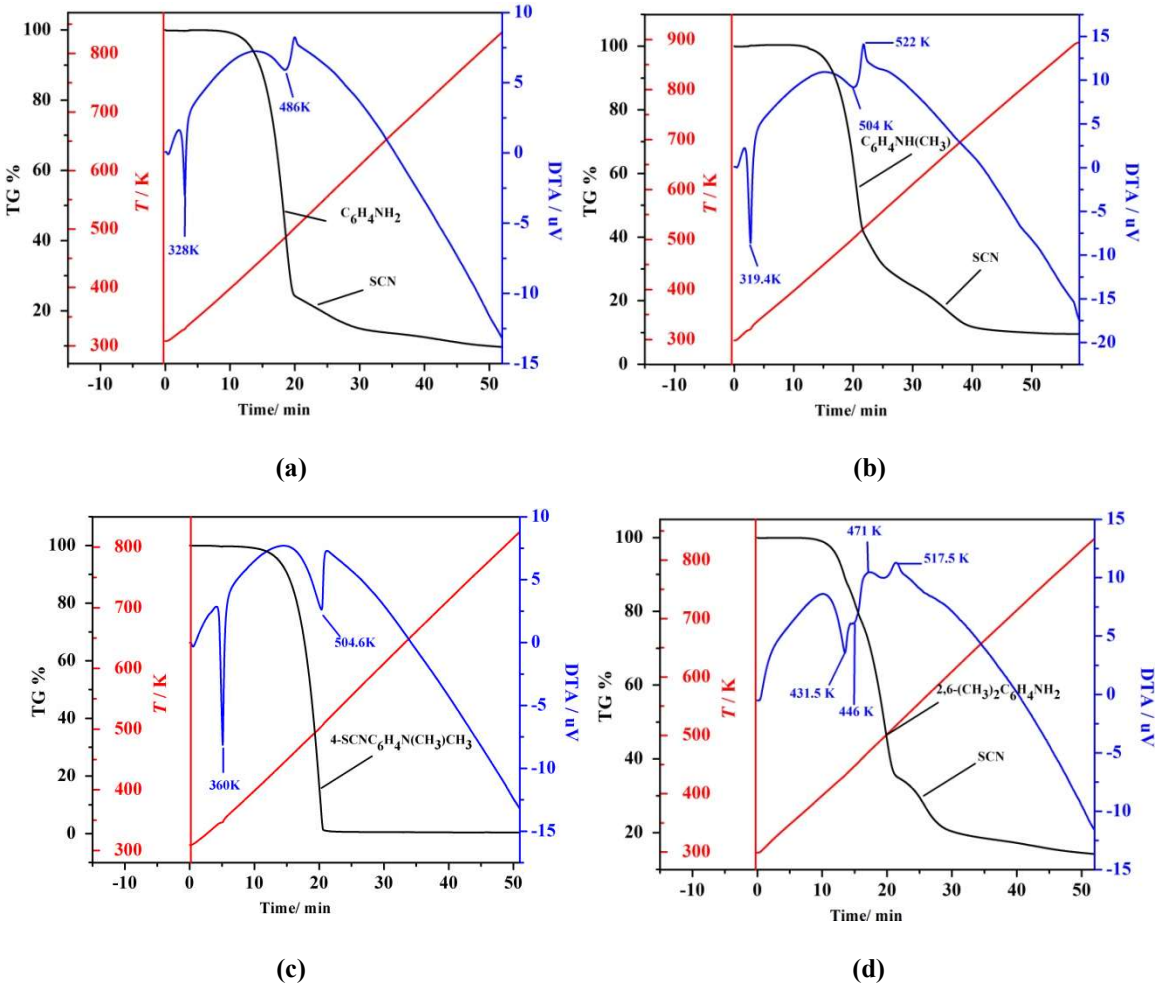


**Fig. 7.10:TG-DTA of compounds (a) 1, (b) 2, (c) 3 and (d) 4**

The aniline moiety from compounds decomposed gradually in the range of 387-502 K for **1** (Obsd. 63.1%, Calcd. 62.25%), 403-555 K for **2** (Obsd. 66.01%, Calcd. 65.24%) and 384-515K for **4** (Obsd. 67.00%, Calcd. 67.98%) while whole molecule get decomposed in the range of 390-531 K for **3** (Obsd. 100%, Calcd.100%).

The DTA curves for all compounds **1** (328 K), **2** (319.4 K) and **3** (360 K) showed distinct endothermic phase transition from solid to liquid state, confirmed separately by manually taking melting points. Compounds indicate that the decomposition of the compound took place with one endothermic peak at 486 K for **1**, 504 K for **2** and 504.62 K for **3** corresponding to loss of aniline moiety. Two endothermic effects observed at 431.5 K and 446 K and two exothermic effects at 471 K and 517.5 K in case of **4**.

## 7.5 Crystal structure

### 7.5.1 Single Crystal X-ray Diffraction

Single crystal XRD confirms the formation of compounds and crystals. Results of single crystal X-ray analysis for compounds **1**, **3** and **4** (Figure 7.11 a-b and 7.12) are listed in Table 7.3. All bond length and bond angles are listed in Table 7.4.

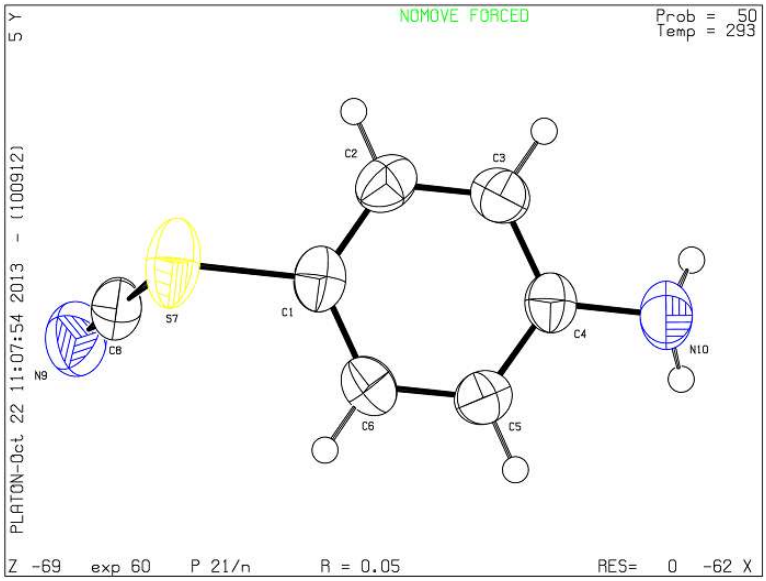


**(a)**

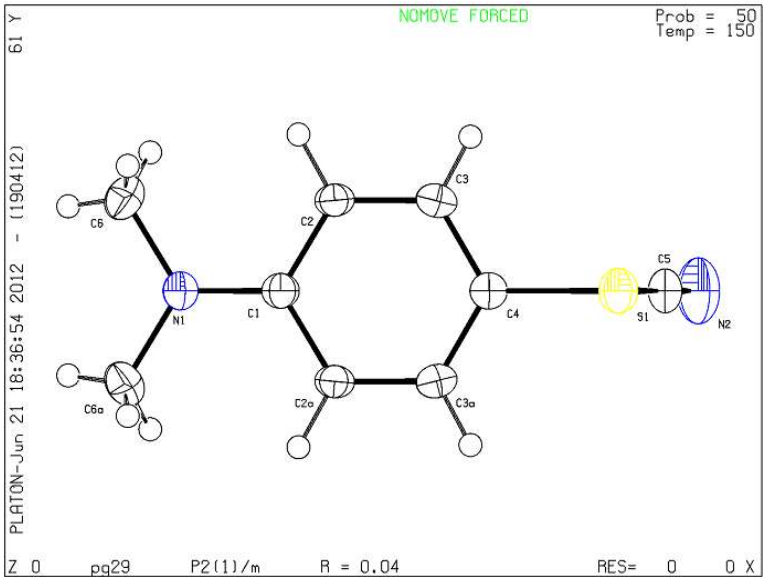


**(b)**

**Fig. 7.11: Molecular view of compounds 1 (a) and 3 (b) having thermal ellipsoid is drawn at the 50% probability level**

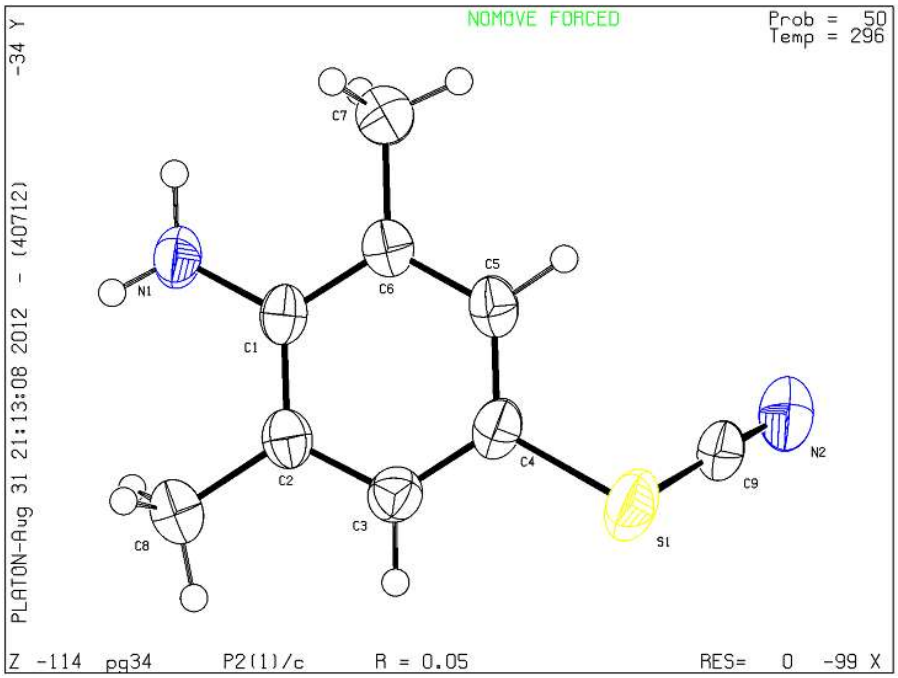


**Fig. 7.12: Molecular view of compounds 4 having thermal ellipsoid is drawn at the 50% probability level**

**Table 7.3: Crystallographic data and structure refinements for compounds 1, 3 and 4 at RT**

| Compounds | 1 | 3 | 4 |
|---|---|---|---|
| **Empirical formula** | $C_7H_6N_2S$ | $C_9H_{10}N_2S$ | $C_9H_{10}N_2S$ |
| **Formula weight** | 150.21 | 178.25 | 178.25 |
| **Wavelength** | 1.54184 Å | 0.71073 Å | 0.71073 Å |
| **Crystal system** | Monoclinic | Monoclinic | Monoclinic |
| **Space group** | *P* 21/*n* | *P* 2(1)/*m* | *P* 2(1)/*c* |
| **Unit cell dimensions** | a = 12.3604(7)Å<br>b = 4.42635(18) Å<br>c = 13.4575(6) Å<br>β= 94.801(5) °. | a = 4.4592(2) Å<br>b = 9.9631(4) Å<br>c = 10.2383(5) Å<br>β= 91.328(4) °. | a = 11.529(2) Å<br>b = 4.2355(8) Å<br>c = 19.235(3) Å<br>β= 106.633(12) °. |
| **Volume** | 733.70(6) | 454.74(4) $Å^3$ | 899.9(3) $Å^3$ |
| **Z** | 4 | 2 | 4 |
| **Density (calculated)** | 1.360 $Mg/m^3$ | 1.302 $Mg/m^3$ | 1.316 $Mg/m^3$ |
| **Absorption coefficient** | 3.243$mm^{-1}$ | 0.299 $mm^{-1}$ | 0.303 $mm^{-1}$ |
| **Reflections collected** | 2157 | 4080 | 7578 |
| **Independent reflections** | 1441[R(int) = 0.0173] | 1838 [R(int) = 0.0175] | 2330 [R(int) = 0.0424] |
| **Refinement method** | Full-matrix least-squares on $F^2$ | Full-matrix least-squares on $F^2$ | Full-matrix least-squares on $F^2$ |
| **Data / restraints / parameters** | 1441 /0/ 93 | 9128 / 1 / 392 | 2330 / 0 / 149 |
| **Goodness-of-fit on F2** | 1.049 | 1.032 | 1.042 |
| **Final R indices [I>2sigma(I)]** | $R_1$ = 0.0465, $wR_2$ = 0.1289 | R1 = 0.0439, wR2 = 0.1300 | R1 = 0.0521, wR2 = 0.1272 |
| **R indices (all data)** | $R_1$ = 0.0545, $wR_2$ = 0.1408 | R1 = 0.0500, wR2 = 0.1353 | R1 = 0.0862, wR2 = 0.1426 |
| **CCDC** | 967792 | 916620 | 916617 |

4-thiocyanato aniline (**1**) crystallizes into $P2_1/n$, *N*, *N*-dimethyl-4-thiocyanato aniline (**3**) into *P*2(1)/*m* while 2,6-dimethyl-4-thiocyanato aniline (**4**) crystallizes into *P*21/*c* space group. We were unable to grow crystals suitable for single crystal X-ray analysis for compound (**2**).

The structural factors which will play important role in present radiative studies are discussed below.

**Amino Twist Angle $\theta$:** The amino twist angle $\theta$ is angle between two planes passing through (C(2) C(1) N(1) + C(6) C(1) N(1). For compound **1**, a small amino twist angle $\theta$= 3.76º was observed. The presence of methyl substituent at amino group substantially decreases this amino twisting to 0.47º in compound **3**. The methyl groups at 2, 6 positions in phenyl ring does not cause much steric hindrance results into twist angle $\theta$= 3.15º.

**Amino phenyl bond N(1)-C(1)** : The length of the bond between the amino nitrogen and the phenyl ring for compounds **1**, **3** and **4** around 1.377Å. Slightly longer bond length of compound **1** and **4** caused by the larger amino twist and thiocyanato angle.

**Thiocyanato angle**: The thiocyanato moiety (S(1) C(7) N(2)) is not planar (quasi linear) in all compounds. It is making an angle of 178.4º, 178.7º and 176.7º in **1**, **3** and **4,** respectively. The thiocyanato angle is angle between two planes passing through S(1) C(7) N(2) + C(3) C(4) C(5). We observe changes in this angle in present set of compounds. In compound **1**, thiocyanato angle is 74.16º, in compound **3** it is 90º while in compound **4** it is 67.44º. From this it is clear that alkyl substitution on amino group make thiocyanato moiety orthogonal to phenyl ring contrarily to substitution on phenyl ring.

The angle between planes passing through C(3)-C(4)-S(1) and C(5)-C(4)-S(1) is around 120º for 1 and 2 and changes considerably for compound **4** (118.42º and 120.89º). Reason behind this might be due to increase in steric hindrance on phenyl ring near thiocyanato moiety to bent down towards phenyl ring planarity which create strain in ring.

**Table 7.4: All bond lengths and bond angles data at Ground State Structure of compounds 1, 3 and 4 from X-ray Crystal Analysis**

| | 1 | 3 | 4 |
|---|---|---|---|
| S(1)-C(4) | 1.780 | 1.774 | 1.785 |
| S(1)-C(7) | 1.693 | 1.698 | 1.678 |
| C(7)-N(2) | 1.139 | 1.142 | 1.145 |
| C(1)-N(1) | 1.383 | 1.359 | 1.390 |
| C(1)-C(2) | 1.394 | 1.385 | 1.406 |
| C(2)-C(3) | 1.373 | 1.386 | 1.385 |
| C(3)-C(4) | 1.386 | 1.389 | 1.382 |
| C(4)-C(5) | 1.384 | 1.392 | 1.379 |
| C(5)-C(6) | 1.378 | 1.389 | 1.386 |
| C(6)-C(1) | 1.388 | 1.384 | 1.406 |
| C(3)-C(4)-S(1) | 119.94º | 120.40º | 118.42º |
| C(5)-C(4)-S(1) | 120.34º | 120.40º | 120.89º |
| S(1)-C(7)-N(2) | 178.43º | 178.73º | 176.74º |
| C(1)-C(2)-C(3) | 121.08º | 121.00º | 119.03º |
| C(2)-C(3)-C(4) | 119.93º | 120.71º | 120.53º |
| C(3)-C(4)-C(5) | 119.66º | 119.10º | 120.62º |
| C(4)-C(5)-C(6) | 120.15º | 120.71º | 120.42º |
| C(5)-C(6)-C(1) | 120.83º | 121.00º | 119.16º |
| C(6)-C(1)-C(2) | 118.33º | 117.46º | 120.19º |
| C(2)-C(1)-N(1) | 121.45º | 121.27º | 119.94º |
| C(6)-C(1)-N(1) | 120.11º | 121.27º | 119.80º |
| C(1)-N(1)-C(8), C(1)-N(1)-C(8)’ | | 120.99º | |
| C(8)-N(1)-C(8’) | | 117.45º | |

## 7.6 Spectral Information

### 7.6.1 UV-Visible Spectra and fluorescence spectra:

The absorption spectra of the four compounds at 25º C are tabulated in Table 7.5 with increase in polarity of solvents.

**Table 7.5: Absorption spectra values of $\lambda_{max}$ of compounds 1, 2, 3 and 4 in different solvents**

| Compounds/ Solvents | $CHCl_3$ (nm) | $CCl_4$ (nm) | DCM (nm) | EtOAc (nm) | ACN (nm) | MeOH (nm) |
|---|---|---|---|---|---|---|
| **1** | 259 ($\lambda_{max}$) 299 | 267 ($\lambda_{max}$) 303 | 259 ($\lambda_{max}$) 297 | 275 ($\lambda_{max}$) | 211, 298 260 ($\lambda_{max}$) | 211 262 ($\lambda_{max}$) |
| **2** | 281 ($\lambda_{max}$) | 279 ($\lambda_{max}$) 319 | 280 ($\lambda_{max}$) 321 | 263 ($\lambda_{max}$) | 208, 298 279 ($\lambda_{max}$) | 213 278 ($\lambda_{max}$) |
| **3** | 283 ($\lambda_{max}$) | 278 ($\lambda_{max}$) 321 | 281 ($\lambda_{max}$) 321 | 261 ($\lambda_{max}$) 294 | 209, 298 281 ($\lambda_{max}$) | 209 278 ($\lambda_{max}$) |
| **4** | 258 ($\lambda_{max}$) 306 | 265 ($\lambda_{max}$) 296 | 259 ($\lambda_{max}$) 292 | 262 ($\lambda_{max}$) 299 | 217, 262 ($\lambda_{max}$), 294 | 217, 261 ($\lambda_{max}$), 292 |

Compounds differ by the presence of a methyl group on amino group and/or on the phenyl ring. Yet they exhibit markedly different absorption spectra. An inspection of Table 7.5 reveals that introduction of an alkyl group leads to profound changes in the spectral properties. The absorption spectra are normally blue shifted in polar aprotic and protic solvents while red shifted in non polar solvents. In general absorption maxima in case of compounds 1 and 4 are blue shift of ~ 15-20 nm in the absorption maxima was observed for **2** and **3** while red shift of ~ 15 nm for compounds **1** and **4**. In polar solvents, methanol and acetonitrile, a band appear in the high energy region (around 210 nm) along with molecular absorption (in the range of 260 to 300 nm), these two transitions can be correlated to ground state (S0) to excited state singlet states S1 and S2, respectively.

DMABN showed dual fluorescence and strong red-shift in long-wavelength fluorescence, $\boldsymbol{F_A}$, with increase in polarity of the solvent. Figures 7.13-7.18 show clearly that compounds **1-4** (0.25 mM) also show dual fluorescence behavior at room temperature and in variety of solvents. Summary for each compounds behavior in different solvent is tabulated in Table 7.6. It denotes the long wavelength fluorescence as the $\boldsymbol{F_A}$ band, the short wavelength one as $\boldsymbol{F_B}$. $\boldsymbol{F_B}$ and $\boldsymbol{F_A}$ emission bands differ in their nature, $\boldsymbol{F_B}$ band correspond to π* to π transition which is delocalized over whole conjugated π-electronic system while $\boldsymbol{F_A}$ band represents a typical CT fluorescence. One can observe $\boldsymbol{F_A}$ fluorescence behavior analogous to DMABN and suggest emission from a twisted intramolecular charge-transfer (TICT) state. Interestingly, structural similarity between compounds **1** and **4** resulted in quite comparable photo-physical behavior.

**Table 7.6: Emission spectra values of compounds 1, 2, 3 and 4 in different solvents**

| Compounds / Solvents | | $CHCl_3$ (nm) | $CCl_4$ (nm) | DCM (nm) | EtOAc (nm) | ACN (nm) | MeOH (nm) |
|---|---|---|---|---|---|---|---|
| **1** | **B** | 357 | 349 | 354 | 354 | 354 | 355 |
| | **A** | 466 | 435, 469 | 435, 465 | 440 | 469 | 467 |
| **2** | **B** | 354 | 357 | 354 | 356 | 351 | 359 |
| | **A** | 433 | 445 | 435 | 434, 468 | 416, 440 | 434,463 |
| **3** | **B** | 363 | 363 | 358 | 359 | 366 | 368 |
| | **A** | 423 | 447 | 430 | 440 | 423, 462 | 441 |
| **4** | **B** | 348 | 334 | 339 | 346 | 342 | 350 |
| | **A** | 415 | 468 | 416 | 425, 466 | 428 | 437 |

### 7.6.1.1 Non Polar Solvents

#### 7.6.1.1.1 Chloroform:

Compound **1** and 4 showed absorbance maxima near 259 nm and lower energy band or hump around 300 nm (i.e. ground state singlet S0 to the excited state singlet's S1 and S2). For compound **2** and **3** absorption spectra's are red shifted (281 and 283nm) and without resolving lower energy band. That means methyl group addition on amino group leads to red shift in absorbance maxima. The order of the energies of the first absorption band $\upsilon^{\sim max}$ (S1, abs) for compounds **1-4** in chloroform (Table 7.5) is: **2** ≈ **3** > **1** ≈ **4**.

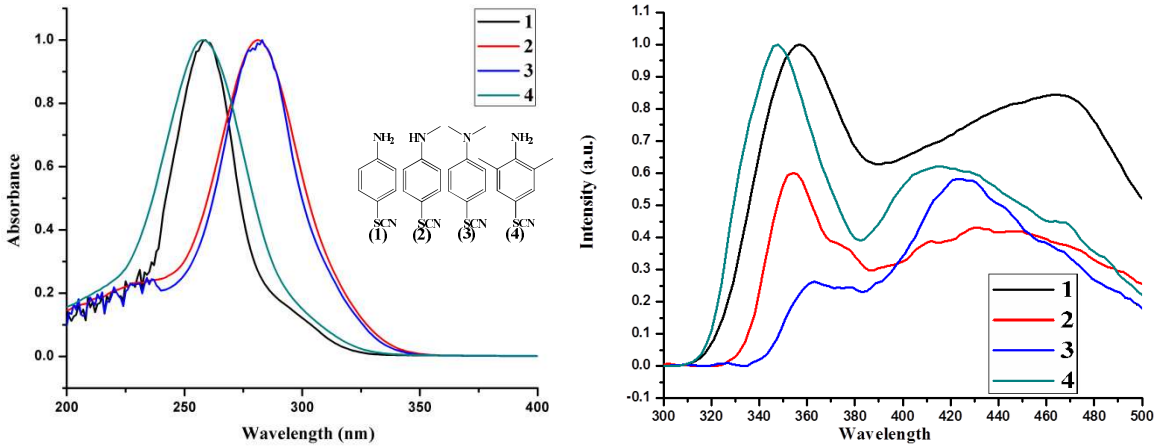


**Fig. 7.13: Normalized absorption (Abs) and fluorescence spectra of the four thiocyanato aniline and its derivatives in chloroform (a) at 25°C**

The fluorescence spectra of compounds **1-4** in chloroform (25°C) showed dual emission behavior. Major band in Compounds **1**, **2** and **4** is $\boldsymbol{F_B}$ while it is $\boldsymbol{F_A}$ for compound **3**. Ideally origin of $\boldsymbol{F_B}$ band and $\boldsymbol{F_A}$ band reside in π to π* based transition and ICT based fluorescence, respectively. In compound **1**, **2** and **4**, emission intensity of $\boldsymbol{F_B}$ steadily decreased and that of $\boldsymbol{F_A}$ steadily increased. This means, addition of methyl substituent on the amino group can be measured by observing changes in the intensity ratio $\boldsymbol{F_A/F_B}$. This assumption can be perfectly extrapolated to compound **3**, where intensity ration of $\boldsymbol{F_A/F_B}$ is exactly reversed. This behavior is quite similar to the set of 4-carbonyl substituted aniline derivatives [16].

**7.6.1.1.2 $CCl_4$:**

In $CCl_4$ solvent, compound **1** and **4** showed bathochromic shift (red shift) at 267 and 265 nm respectively with lower energy band separation. Contrary, compound **2** and **3** showed slight hypsochromic shift at 279 and 278 nm with separation of lower energy band. The order of the energies of the first absorption band $\upsilon^{\sim max}$ (S1, abs) for compounds **1**-**4** in $CCl_4$ (Table 7.5) is: **2** ≈ **3** > **1** > **4**.

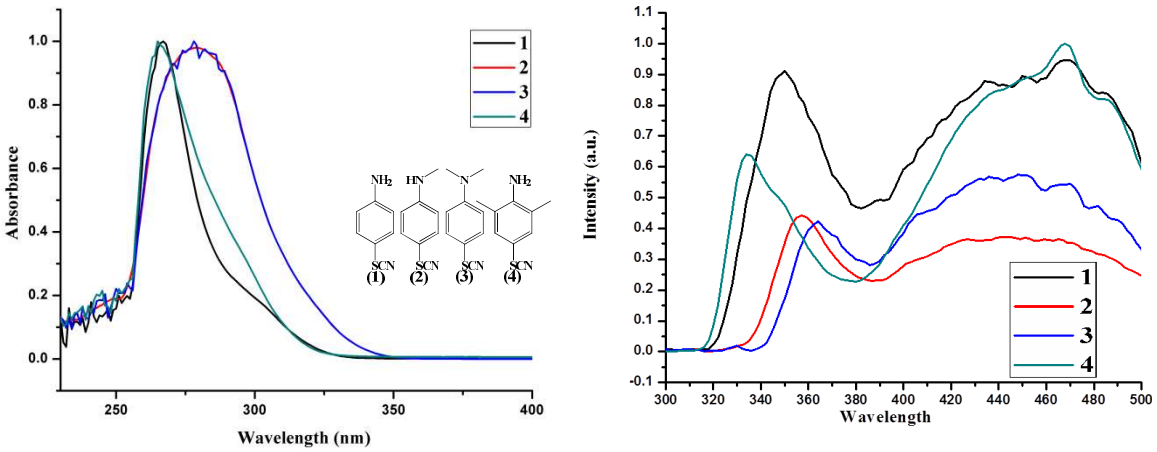


**(b)** **(b)**

**Fig. 7.14: Normalized absorption (Abs) and fluorescence spectra of the four thiocyanato aniline and its derivatives in $CCl_4$ (b) at 25°C**

$CCl_4$ having symmetrical geometry, hence it is preferable non polar solvent in which single crystal properties of compounds can be correlated directly with emission study. The fluorescence spectra of compounds **1**-**4** in $CCl_4$ at 25°C consist of a dual emission bands and follow TICT mechanism. Compound **2** showed $\boldsymbol{F_B}$ band and $\boldsymbol{F_A}$ band almost in 1:1 intensity while in compounds **1**, **3** and **4** it is observed that $\boldsymbol{F_A}$ band intensity increased. These results are in accordance with angle of thiocyanato results and confirm the role of it in $\boldsymbol{F_A}$ band emission.

### 7.6.1.2 Polar aprotic solvents

#### 7.6.1.2.1 DCM:

The order of the energies of the first absorption band $\upsilon^{\sim max}$ (S1, abs) for compounds **1** - **4** in chloroform (Table 7.5) is: **2** ≈ **3** > **1** ≈ **4**. A similar order of the energies of the first absorption band has been obtained for compounds **1**-**4** in DCM as that of chloroform suggest not much change happened in stabilizing polar state.

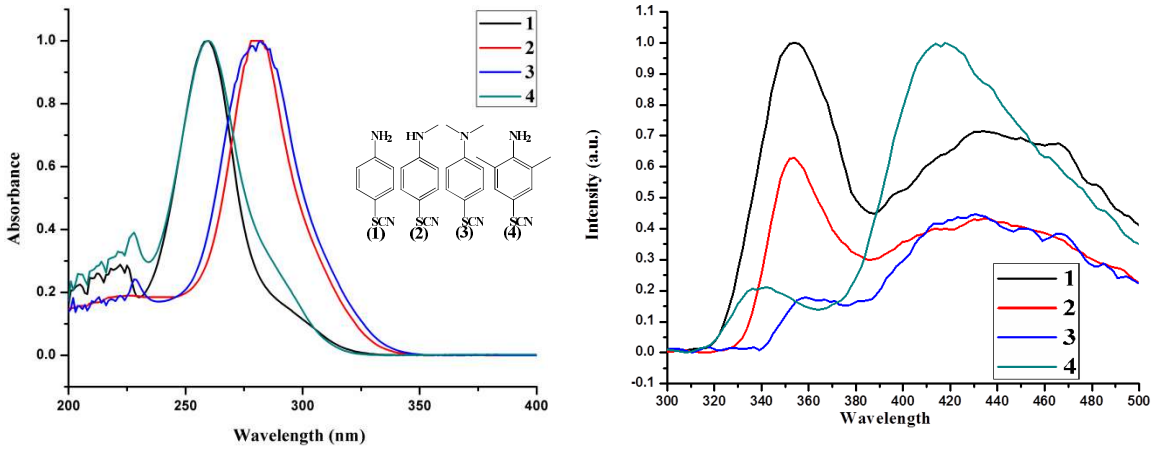


(c) (c)

**Fig. 7.15: Normalized absorption (Abs) and fluorescence spectra of the four thiocyanato aniline and its derivatives in DCM (c) at 25ºC**

The fluorescence spectra of compounds **1**-**4** in DCM at 25°C consist of a dual emission bands and follow TICT mechanism. Compounds **1** and **2** showed major $\boldsymbol{F_B}$ band corresponding to a typical π* to π transition while compound **3** and **4** showed $\boldsymbol{F_A}$ band representing a typical CT fluorescence. In compound **1**, **2** and **3**, emission intensity of $\boldsymbol{F_B}$ steadily decreased and that of $\boldsymbol{F_A}$ increased affecting intensity ratio $\boldsymbol{F_A/F_B}$ as methyl substituent increase on amino group. Surprisingly compound **4** showed presence of major $\boldsymbol{F_A}$ band similar to compound **3** in which no methyl substitution on amino group. This can be attributed to rotation of thiocyanato moiety which might make 90º angles to phenyl ring.

**7.6.1.2.2 Ethyl acetate:**

In ethyl acetate, compound **1** showed bathochromic shift at 275 nm while compound **4** does not showed any remarkable change in wavelength. Contrary, compounds **2** and **3** showed remarkable hypsochromic shift at 263 and 261 nm suggesting stabilization of polar state in excited state with increased polarity. The order of the energies of the first absorption band get changed and $\upsilon^{\sim max}$ (S1, abs) for compounds **1 - 4** in ethyl acetate (Table 7.5) is: **1** > **2** > **3** ≈ **4**.

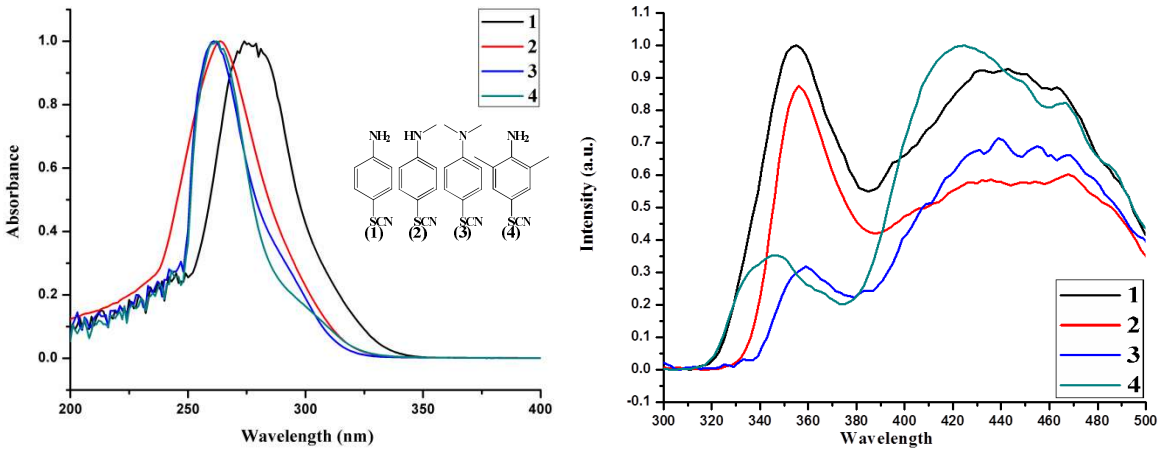


**(d)** **(d)**

**Fig. 7.16: Normalized absorption (Abs) and fluorescence spectra of the four thiocyanato aniline and its derivatives in ethyl acetate (d) at 25ºC**

The fluorescence spectra of compounds **1 - 4** in ethyl acetate at 25°C consist of a dual emission bands and follow TICT mechanism. Compounds showed similar emission behavior as that of DCM solvent.

### 7.6.1.2.3 Acetonitrile:

With increase in polarity substantial changes occurred in absorption spectra. All compounds showed two major absorption bands attributed to S0 to S1 and S0 to S2 transitions. Compound **1**, **2** and **3** showed similar absorbance maxima as that of in chloroform solvent with additional highly hypsochromic band of almost same absorbance at 211, 208 and 209 nm respectively. Compound **4** showed contrary highly hypsochromic absorbance maxima at 217 nm and an additional band at 262 nm. Highly hypsochromic band can be attributed to π-π* transition and higher wavelength band due to π-π*/ n-π* transition. The order of the energies of the first absorption band get changed and $\upsilon^{\sim max}$ (S1, abs) for compounds **1**-**4** in acetonitrile (Table 7.5) is: **3** > **2** > **1** > **4**.

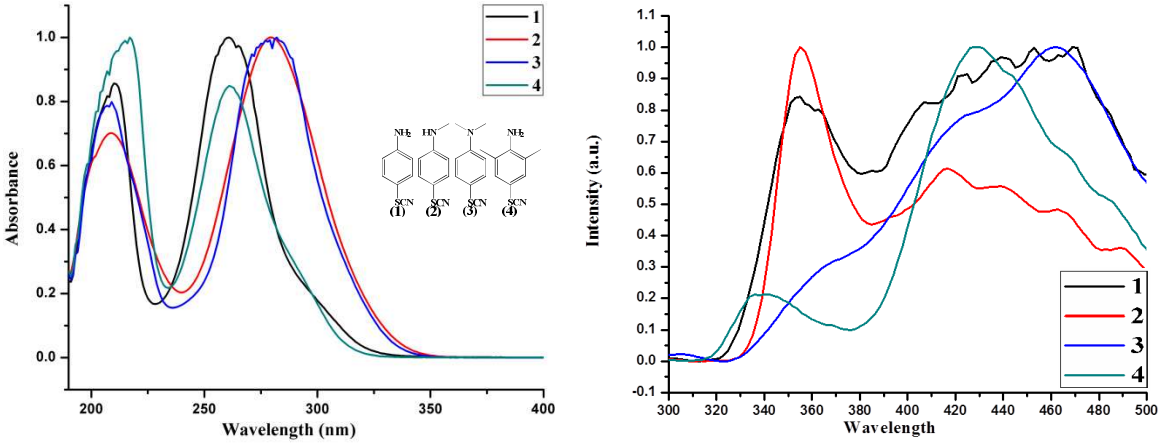


**Fig.7.17: Normalized absorption (Abs) and fluorescence spectra of the four thiocyanato aniline and its derivatives in acetonitrile (e) at 25°C**

The fluorescence spectra of compounds **1**-**4** in ACN at 25°C consist of a dual emission bands and follow TICT mechanism. Compound **2** showed major $\boldsymbol{F_B}$ band corresponding to a typical π* to π transition while compound **1** showed $\boldsymbol{F_B}$ band and $\boldsymbol{F_A}$ band almost in 1:1 intensity. Compound **3** showed only $\boldsymbol{F_A}$ band representing a typical CT fluorescence. This enhancement in ICT efficiency is caused by the introduction of a dimethyl substituent into the amino group. Here twisting of dimethyl amino group might occurred along with rotation of –SCN moiety which may give only $\boldsymbol{F_A}$ band. Such a large twist angle leads to an efficient electronic decoupling between the amino and –SCN moieties. The excited state might be stabilized by polar acetonitrile solvent. Compound **4** showed similar emission behavior as that of in DCM and ethyl acetate.

### 7.6.1.3 Polar protic solvent

#### 7.6.1.3.1 Methanol:

A similar order of the energies of the first absorption band has been obtained for compounds **1-4** in highly polar solvent methanol as that of ACN suggesting more polar solvents stabilized polar state. The absorption spectra consist of two bands, again attributed to S0 to S1 and S0 to S2 transitions. The order of the energies of the first absorption band get changed and $\upsilon^{\sim max}$ (S1, abs) for compounds **1** - **4** in acetonitrile (Table 7.5) is: **3** ≈ **2** > **1** > **4**.

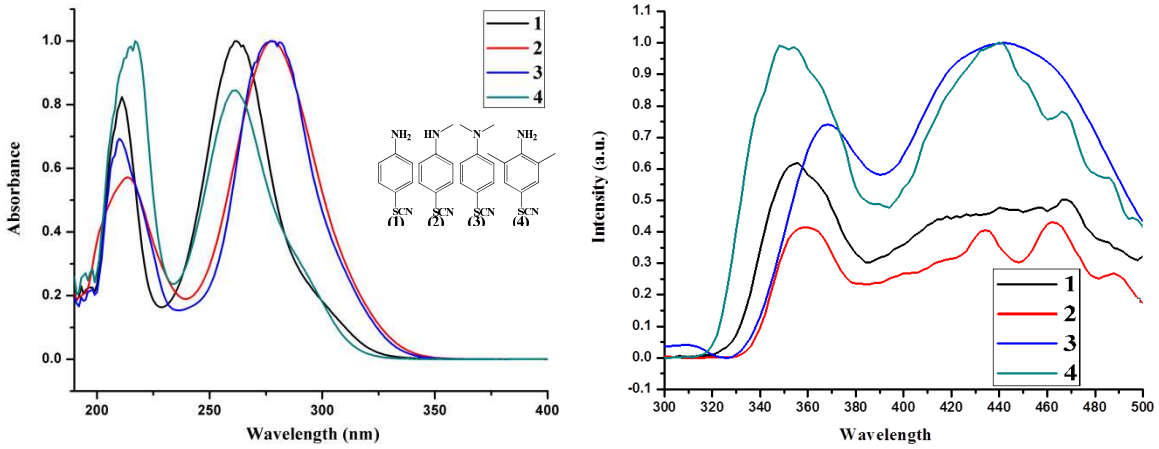


**Fig.7.18: Normalized absorption (Abs) and fluorescence spectra of the four thiocyanato aniline and its derivatives in methanol (f) at 25ºC**

The fluorescence spectra of compounds **1** - **4** in methanol at 25°C consist of a dual emission bands and follow TICT mechanism. Compounds **1**, **2** and **4** showed $\boldsymbol{F_B}$ band and $\boldsymbol{F_A}$ band almost in 1:1 intensity. Compound **3** showed major $\boldsymbol{F_A}$ band representing a typical CT fluorescence. Polar solvent might be stabilizing the SCN moiety as well as dimethyl amino twisting state by solvation i.e. strong hydrogen bonding due to which the rotation of it might get hindered or minimized results into both $\boldsymbol{F_B}$ and $\boldsymbol{F_A}$ bands. With compounds **1**, **2** and **3**, in contrast, an additional fluorescence band is present at the low-energy side of the ICT emission and the band is attributed to the ICT state.

# Part II

## Studies on 4-thiocyanato aromatic amine salts

## 7.7 Experimental

### 7.7.1 Materials and Methods:

All chemicals and solvents were of analytical grade reagents. Conc. HCl was from Loba chemie; doubly deionized water and ethyl alcohol (Baroda Chemicals) were used without further purification.

### 7.7.2 Syntheses of 4-thiocyanato aniline salts

A general methodology of 4-thiocyanato aniline nitrate (**5**) and 4-thiocyanato aniline hydrochloride (**6**) preparation/syntheses is mentioned in scheme-7.5 and scheme-7.5 respectively.

**Scheme 7.5:**

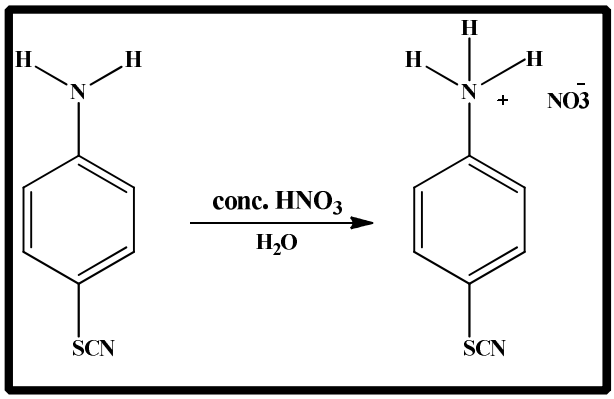


**Scheme 7.6:**

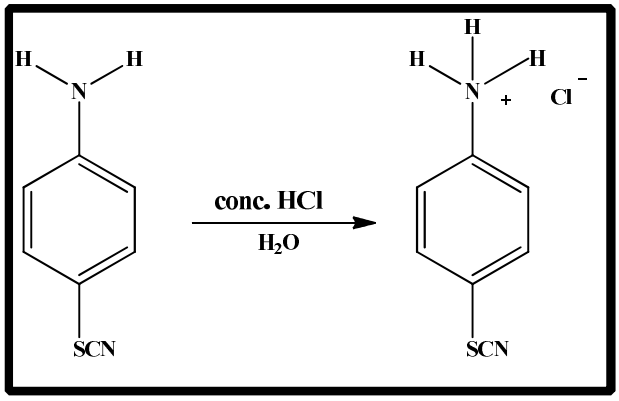

### 7.7.3 Experimental Procedure:

A series of anilinium nitrate derivatives were prepared by the dropwise addition of excess concentrated hydrochloric acid (0.90 mL) /nitric acid (0.92 mL) to a solution of 4-thiocyanato aniline-**1** (0.1 gm) in 10 ml water. Slow evaporation of the aqueous solution at room temperature gave colorless crystals.

Recrystallizations were performed to increase purity using doubly deionized water which on slow evaporation gave good quality of single crystals.

The percentage yield obtained for 4-aniline thiocyanato hydrochloride and Derivative are shown in Table 7.7.

**Table 7.7: Percentage yield of $HNO_3$/ HCl salts of 4-thiocyanato aniline**

| Compounds | % Yield | Colour |
|---|---|---|
| **4-SCN An $HNO_3$ (5)** | 100 % | Colorless |
| **4-SCN An HCl (6)** | 100 % | Colorless |

## 7.8 Result and Discussions

### 7.8.1 FT-IR:

FT-IR spectra for a series of 4-thiocyanato aniline salts (**5** and **6**) were recorded in the range of 4000 - 400 $cm^{-1}$ at RT.

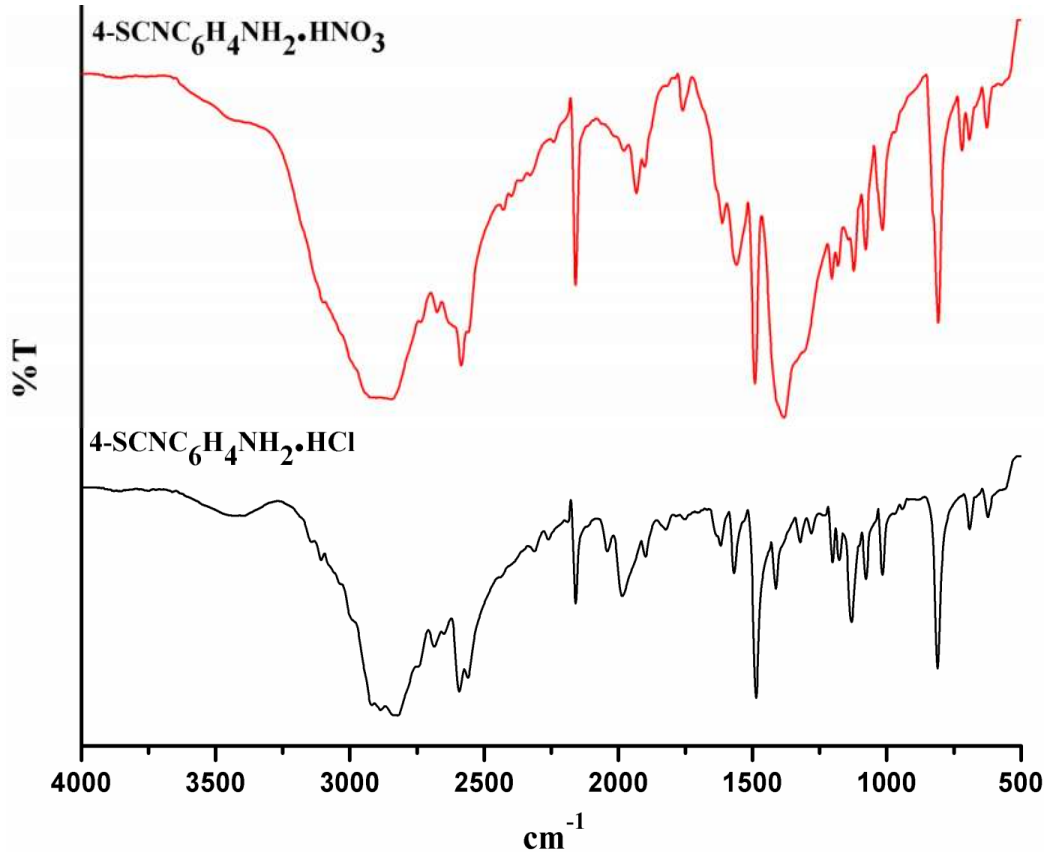


**Fig. 7.19: FT-IR of compounds 5 and 6**

**Compound 5- FT-IR (KBr):**: 3101(m), 3032(w), 2925(vs), 2843 (vs), 2732 (m), 2675 (m), 2634 (m), 2585 (s), 2556 (w), 2429(w), 2396 (w), 2359( w), 2326(w), 2240(w), 2162(ssh), 1982(w), 1932 (m), 1904(m), 1820(w), 1760 (s), 1640 (w), 1615(m), 1558(s), 1491 (ssh), 1386(vs), 1308(vs), 1206 (m), 1181 (m), 1150(w), 1121 (s), 1079 (s), 1035 (m), 1015(s), 963(w), 934(w), 829(s), 807(vssh), 720 (s), 691 (m), 628(s), 572(w) and 542 (w) $cm^{-1}$.

**Compound 6- FT-IR (KBr):** 3143(m), 3105 (m), 3001(s), 2922 (vs), 2884 (vs), 2827 (vs), 2744 (s), 2687 (s), 2649 (m), 2594 (vs), 2561(vs), 2310 (m), 2260 (s), 2186 (w), 2158 (ssh), 2043 (s), 1987 (s), 1898(m), 1822 (m), 1751(w), 1638(m), 1618(m), 1568 (s),

1529 (w), 1486 (ssh), 1412 (s), 1382 (w), 1322 (m), 1280 (w), 1233(w), 1201 (s), 1176 (s), 1131 (ssh), 1099 (w), 1078 (s), 1039 (w), 1015 (s), 968 (w), 940 (w), 810 (vssh), 690 (s), 623 (s) and 555 (w) $cm^{-1}$.

Strong broad band for N-H (-$NH^{3+}$ group) stretching vibrations were observed in the region 3135-2600 $cm^{-1}$ for compound 5 and 3250 - 2600 cm-1 for compound 6 due to the continuous series of overlapping bands, combination bands and overtone bands. The band at 2634 and 2649 $cm^{-1}$ were assigned to the Fermi resonance of combination bands of (deformation and rocking modes) N-H of -$NH_3$ group for **5** and **6** respectively. Modes observed at 2162 and 2158 $cm^{-1}$ were assigned to cyano frequencies which increase as compared to their parent compound **1**. C-H ring stretching modes were observed at the range of 1640-1412 $cm^{-1}$. The anti-symmetric stretching mode for nitrate anion was observed at 1386 $cm^{-1}$ while symmetric stretching mode at 1491 $cm^{-1}$. Out-of-plane bending was observed at 807 $cm^{-1}$ while in-plane-bending mode at 720 $cm^{-1}$. Bending and symmetric deformation observed around 1650-1608$cm^{-1}$ and 1553-1508$cm^{-1}$ respectively. Vibrations observed at 1308 and 1184-1206 $cm^{-1}$ assigned to C-N stretching. Aromatic C-H out of plane deformation and vibrational bands were observed in range of 690-900 $cm^{-1}$.

### 7.8.2 $^1$H NMR spectra

$^1$HNMR data on present series of compounds (**5 and 6**) are presented in Table 7.8 and shown in Figure 7.20 (**5**) and Figure 7.21 (**6**).

**Table 7.8: Details of $^1$H NMR spectra for compounds 5 and 6**

| Compounds | (δ value) $^1$H NMR (d6-DMSO) J coupling in Hz |
|---|---|
| (**5**) | δ 7.067 (br s 3H, $NH_3^+$), 7.088- 7.138 (d, 2H, J = 8.4), 7.551-7.593 (d, 2H, J = 8.0 and 8.8). |
| (**6**) | δ 6.551 (br s 3H, $NH_3^+$), 7.133- 7.153 (d, 2H, J = 8.0), 7.559-7.587 (q, 2H, J = 2.8). |
| (**1**) | δ 5.809 (s 2H, $NH_2$), 6.618-6.639 (q, 2H, J = 2.0 and 4.4), 7.318-7.331 (q, 2H, J = 2.8 and 5.2). |

Formation of 4-thicyanato anilinium salt has been confirmed by $^1$H NMR spectroscopy (Figure 7.20 and 7.21).

It is observed that**,** N–H protons in compound **1** were in high field (δ = 5.809 ppm) which shift to low field in compounds **5** and **6** and showed broad signal between δ = 7.067 ppm and δ =6.551ppm respectively for three proton due to -$NH_3^+$ moiety. The aromatic protons of compound **5** also shift to low field region due to formation of salt and appears at δ = 7.088- 7.138 ppm shows doublet for ortho-hydrogen's while δ = 7.551-7.593 ppm) for the *meta*-protons. Similar observation has been obtained for compound **6**. Aromatic protons showed doublet appear at δ =7.133- 7.153 ppm for ortho-hydrogen and δ =7.318-7.331 ppm for the *meta*-hydrogen.

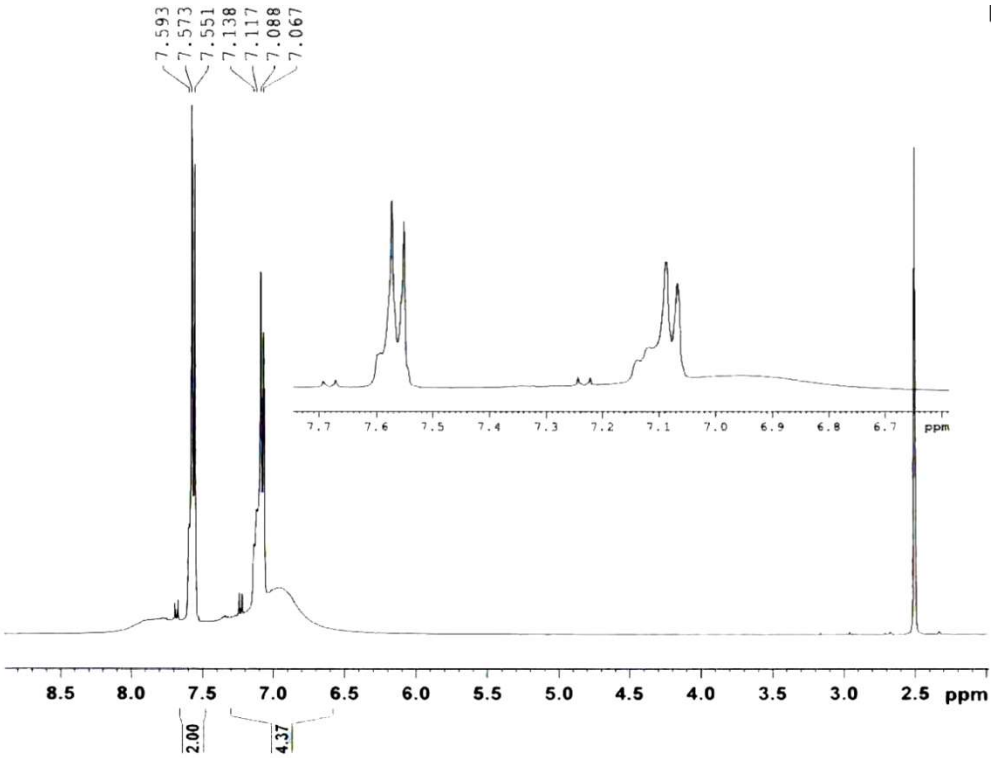


**Fig. 7.20 : $^{1}$H NMR spectra of compound 5**

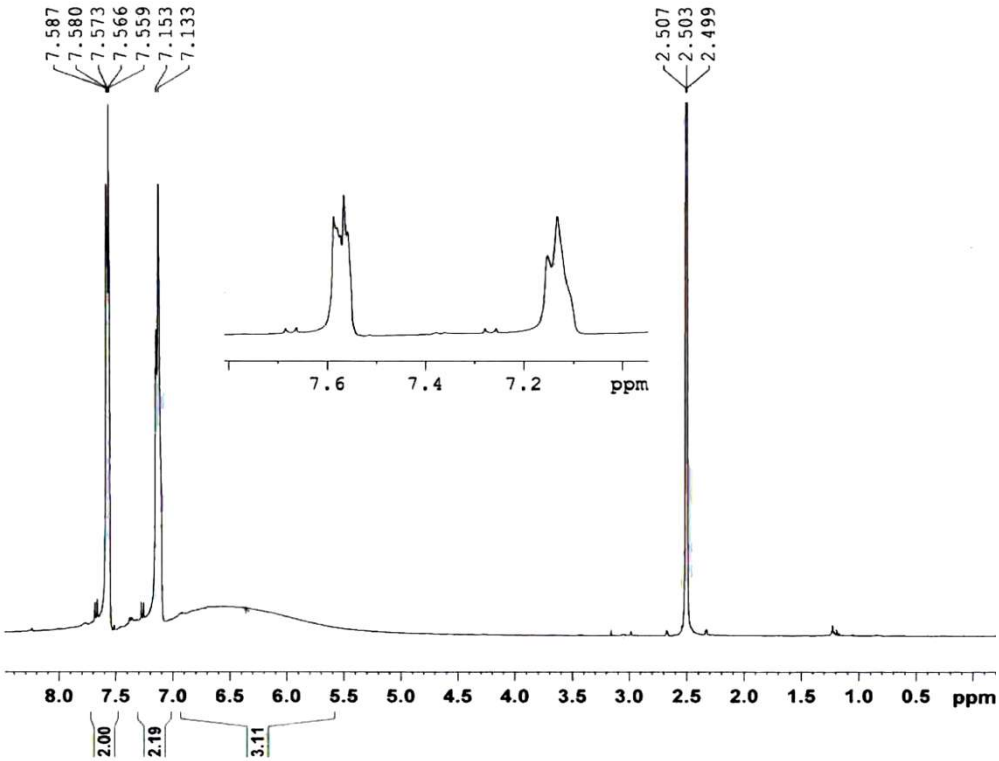


**Fig. 7.21: $^{1}$H NMR spectra of compound 6**

## 7.9 Crystal structure

### 7.9.1 Single Crystal X-ray Diffraction

Single crystal XRD confirms the formation of compounds and crystals. The molecular structure of **5** and **6** are shown in Figure 7.22.

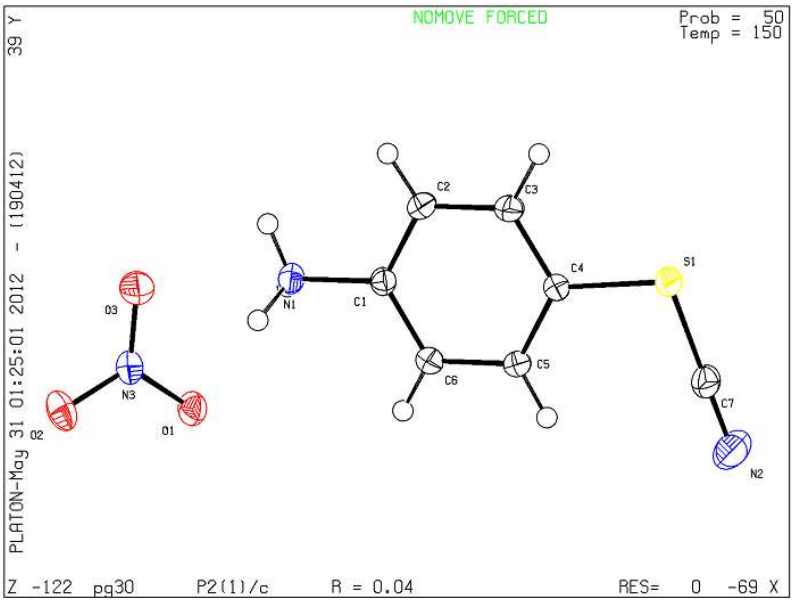


**(a)**

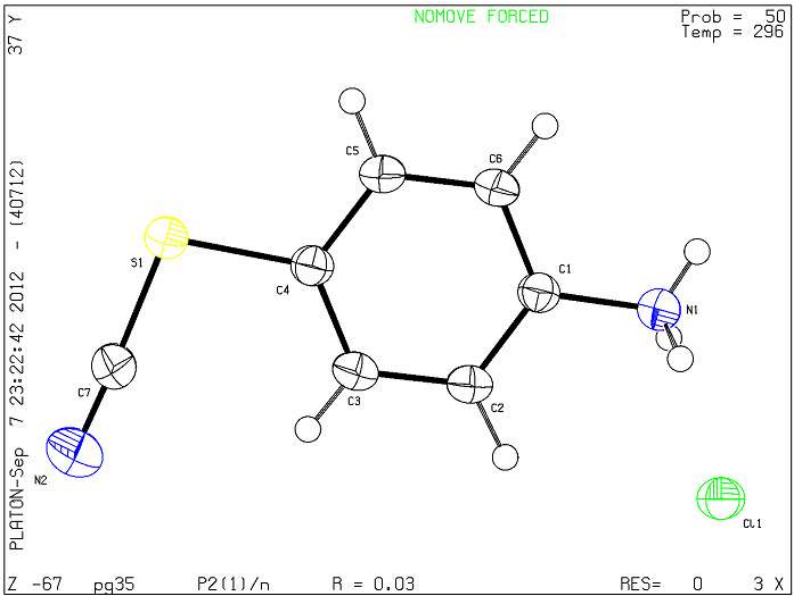


**(b)**

**Fig. 7.22: Molecular view of compounds 5 (a) and 6 (b) having thermal ellipsoid is drawn at the 50% probability level**

**Table 7.9: Crystallographic data and structure refinements for compounds 1, 3 and 4 at RT**

| | **5** | **6** |
|---|---|---|
| **Empirical formula** | $C_7H_7N_3O_3$ S | $C_7$ $H_7$ Cl $N_2$ S |
| **Formula weight** | 213.22 | 186.66 |
| **Wavelength** | 0.71073 Å | 0.71073 Å |
| **Crystal system** | Monoclinic | Monoclinic |
| **Space group** | *P*2(1)/*c* | *P*2(1)/*n* |
| **Unit cell dimensions** | a = 5.7550(1)Å<br>b = 8.0389(1)Å<br>c = 19.6350(4)Å<br>β= 90.944(1)° | a = 5.6625(1)Å<br>b = 17.6032(4)Å<br>c = 8.2897(2)Å<br>β= 92.335(1)° |
| **Volume** | 908.27(3) $Å^3$ | 825.62(3) $Å^3$ |
| **Z** | 4 | 4 |
| **Density (calculated)** | 1.559 $Mg/m^3$ | 1.502 $Mg/m^3$ |
| **Absorption coefficient** | 0.341 $mm^{-1}$ | 0.646 $mm^{-1}$ |
| **Reflections collected** | 8520 | 10963 |
| **Independent reflections** | 3610 [R(int) = 0.0218] | 3271 [R(int) = 0.0246] |
| **Refinement method** | Full-matrix least-squares on $F^2$ | Full-matrix least-squares on $F^2$ |
| **Data / restraints / parameters** | 3610 / 0 / 155 | 3271 / 0 / 128 |
| **Goodness-of-fit on F2** | 1.023 | 1.048 |
| **Final R indices [I>2sigma(I)]** | R1 = 0.0357, wR2 = 0.0903 | R1 = 0.0327, wR2 = 0.0794 |
| **R indices (all data)** | R1 = 0.0481, wR2 = 0.0976 | R1 = 0.0452, wR2 = 0.0861 |
| **CCDC** | 916619 | 916618 |

4-thiocyanato anilinium nitrate (**5**) crystallizes into $P2_1/c$ while 4-thiocyanato anilinium chloride (**6**) crystallizes into *P*21/*n* with *Z*= 4 for both compounds.

**Amino Twist Angle *θ*:** The amino twist angle $\theta$ is angle between two planes passing through (C(2) C(1) N(1) + C(6) C(1) N(1). As compared to parent compound **1** ($\theta$ = 3.76º), compound **5** have small amino twist angle $\theta$= 0.76º while in compound **6** it is perfectly in planar with phenyl ring i.e. angle $\theta$= 0.02º. Formations of salt of compound **1** decrease the angle almost to zero.

**Amino phenyl bond N(1)-C(1)** : The length of the bond between the amino nitrogen and the phenyl ring carbon for compounds **5** and **6** around 1.462 Å. The increment in length is due to formation of salt.

**Thiocyanato angle**: The thiocyanato angle is angle between two planes passing through C(4) S(1) C(7) N(2) + C(3) C(4) C(5). Formation of salts dramatically changed the thiocyanato angle from 74.16º to 7.51 º in compound **5** and 0.57º in compound **6**. In compound **5** substantial hydrogen bonding between nitrate anion and protonated amino group were formed. One unusual S---O supramolecular interaction also formed between –SCN moiety and nitrate anion. This proves that sulphur having electrophilic character. Due to this interaction SCN moiety is not completely planar with phenyl ring. Compound 6 also formed hydrogen bonding between protonated amino group cation and chlorine anion. Table 7.11 shows the hydrogen bonding bond length and bond angles for compound **5** and **6**.

The thiocyanato moiety (S(1) C(7) N(2)) is not planar (quasi linear) in compound 6. Compound **5** formed an angle of 179.14º for **5** and 177.52º for **6**. The angle between planes passing through C(3)-C(4)-S(1)-114.97 and C(5)-C(4)-S(1)- 124.08 are noticeably change for compound **5** while compounds **6** showed C(3)-C(4)-S(1)-115.68 and C(5)-C(4)-S(1)- 123.61 showed similar angles. As steric hindrance at phenyl ring increases due to bent thiocyanato moiety towards phenyl ring planarity which create strain in ring and hence in angles.

**Table 7.10: All bond lengths and bond angles data at Ground State Structure of compounds 1, 5 and 6 from X-ray Crystal Analysis**

| | 1 | 5 | 6 |
|---|---|---|---|
| S(1)-C(4) | 1.780 | 1.781 | 1.783 |
| S(1)-C(7) | 1.693 | 1.675 | 1.682 |
| C(7)-N(2) | 1.139 | 1.143 | 1.142 |
| C(1)-N(1) | 1.383 | 1.461 | 1.461 |
| C(1)-C(2) | 1.394 | 1.414 | 1.381 |
| C(2)-C(3) | 1.373 | 1.382 | 1.382 |
| C(3)-C(4) | 1.386 | 1.394 | 1.387 |
| C(4)-C(5) | 1.384 | 1.394 | 1.390 |
| C(5)-C(6) | 1.378 | 1.382 | 1.385 |
| C(6)-C(1) | 1.388 | 1.414 | 1.382 |
| C(3)-C(4)-S(1) | 119.94 º | 114.97 º | 123.61 º |
| C(5)-C(4)-S(1) | 120.34 º | 124.08 º | 115.69 º |
| S(1)-C(7)-N(2) | 178.43 º | 179.14 º | 177.52 º |
| C(1)-C(2)-C(3) | 121.08 º | 119.60 º | 119.53 º |
| C(2)-C(3)-C(4) | 119.93 º | 119.36 º | 119.50 º |
| C(3)-C(4)-C(5) | 119.66 º | 120.95 º | 120.71 º |
| C(4)-C(5)-C(6) | 120.15 º | 119.39 º | 119.60 º |
| C(5)-C(6)-C(1) | 120.83 º | 119.41 º | 119.21 º |
| C(6)-C(1)-C(2) | 118.33 º | 121.27 º | 121.42 º |
| C(2)-C(1)-N(1) | 121.45 º | 119.74 º | 118.01 º |
| C(6)-C(1)-N(1) | 120.11 º | 118.99 º | 120.58 º |

**Table 7.11:** Hydrogen bonds [Å and °]

| D-H...A | d(D-H) | d(H...A) | d(D...A) | <(DHA) |
|---|---|---|---|---|
| For compound **5** | | | | |
| N(1)-H(1A)...O(1) | 0.912(14) | 1.868(14) | 2.7798(12) | 178.3(13) |
| N(1)-H(1A)...O(3) | 0.912(14) | 2.564(13) | 3.1807(13) | 125.4(10) |
| N(1)-H(1B)...O(2)#1 | 0.903(16) | 1.974(16) | 2.8575(12) | 165.5(14) |
| N(1)-H(1B)...O(3)#1 | 0.903(16) | 2.657(16) | 3.3918(13) | 139.1(12) |
| N(1)-H(1C)...O(1)#2 | 0.866(16) | 2.033(16) | 2.8839(12) | 167.1(14) |
| N(1)-H(1C)...O(2)#2 | 0.866(16) | 2.591(16) | 3.2748(12) | 136.7(12) |
| For compound **6** | | | | |
| N(1)-H(1B)...Cl(1) | 0.851(18) | 2.308(18) | 3.1554(11) | 174.5(16) |
| N(1)-H(1A)...Cl(1)#1 | 0.835(19) | 2.37(2) | 3.1982(10) | 169.8(16) |
| N(1)-H(1C)...Cl(1)#2 | 0.886(17) | 2.348(17) | 3.2054(11) | 162.9(13) |

Symmetry transformations used to generate equivalent atoms:

#1 -x+2,y-1/2,-z+1/2 #2 -x+1,y-1/2,-z+1/2

## 7.10 Spectral Information

### 7.10.1 UV-Visible Spectra and fluorescence spectra:

The absorption spectra of the two compounds at 25º C are tabulated in Table 7.12. Compounds **5** and **6** are differing by the presence of a different anion on protonated amino group. Yet they exhibit same absorption spectra and same $\lambda_{max}$.

**Table 7.12: Absorption spectra values of $\lambda_{max}$ of compounds 5 and 6 in acetonitrile solvent**

| Compounds | Absorption Band (nm) |
|---|---|
| **5** | 330 ($\lambda_{max}$) |
| **6** | 331 ($\lambda_{max}$) |

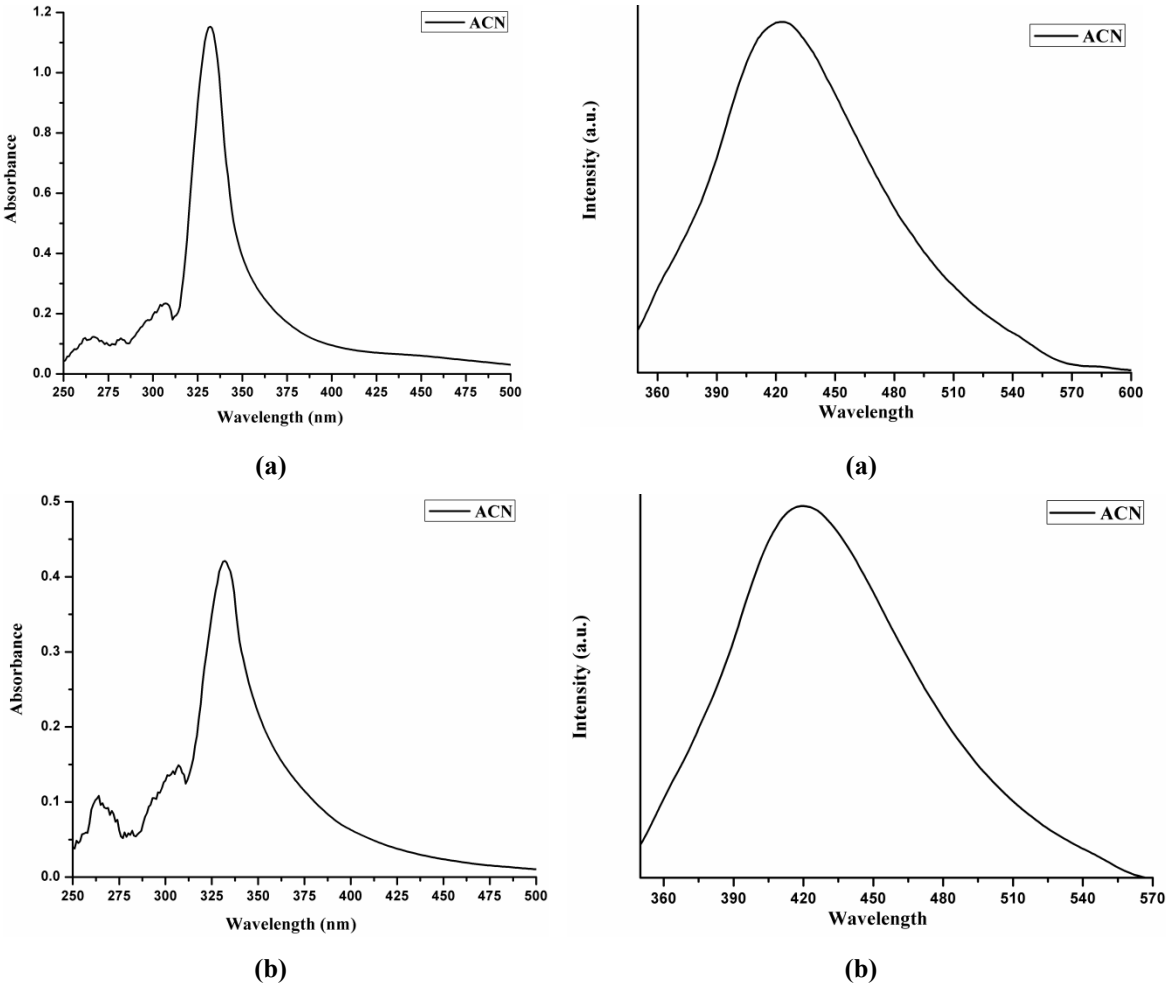


**Fig. 7.23: Absorbance and fluorescence spectra of the compounds 5 (a) and 6 (b) in acetonitrile at 25ºC**

The UV–vis spectra consist of single absorption appears in the near-ultraviolet region. The parent compound i.e. 4-thiocyanato aniline (**1**) displays absorbance maxima at 220 nm and intense broad band maxima ($\lambda_{max}$) at 250 nm in acetonitrile. As salt formation took place absorbance maxima ($\lambda_{max}$) get red shift to 330nm with single absorption band.

The fluorescence spectra of compounds **5** and **6** solutions (0.25 mM) in ACN at 25°C consist of a single emission band. Both compounds **5** and **6** showed band representing a typical locally excited (LE) state fluorescence with red shift of around 80 nm which is in accordance with the absorption spectra. Dual fluorescence gets diminished due to hydrogen bonding which causes –SCN moiety to be planar with phenyl ring. Donor group i.e. amino group is positive in nature hence electron transfer is not possible from it. Hence one can extend role of –SCN moiety in dual fluorescence. If –SCN moiety orthogonal to phenyl ring dual fluorescence will occur on the other hand non planarity of phenyl ring and –SCN moiety leads to single fluorescence. Hence synthesizing bulky groups around phenyl ring to restrict –SCN moiety and –NMe2 group can be planar or orthogonal to phenyl ring will certainly confirm the role of it. To confirm this hypothesis, synthesis of study of following set of compounds will be helpful. These molecules will help to maintain non-planar arrangement of –SCN group with respect to –NMe2 group, by maintaining alternate planar character with phenyl ring

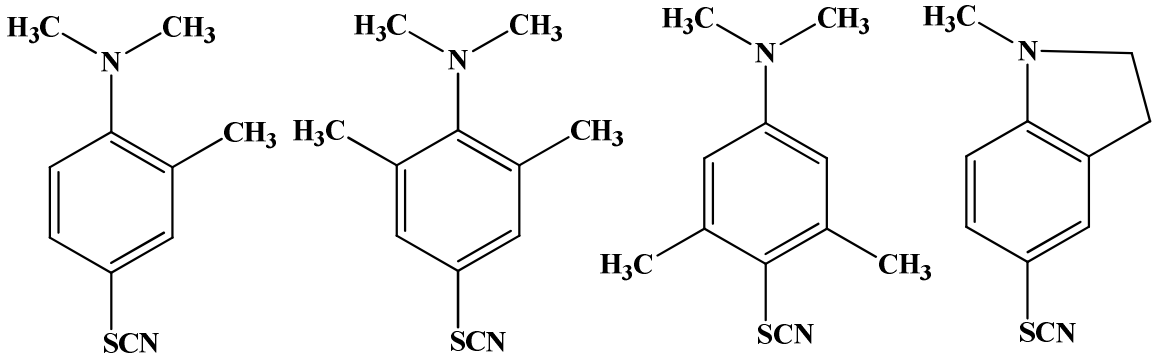

## 7.11 Conclusion

- We successfully synthesized and characterized four new compounds of 4-thiocyanato substituted anilines and two salts using IR, $^{1}H$ NMR and Single crystal XRD.
- Designed a series of smallest aromatic electron donor-acceptor molecules.
- Single crystal XRD showed the rotation of thiocyanato group is dependent on substituent present on amine group and phenyl ring.
- Fluorescence study shows the presence of Dual Fluorescence ($\boldsymbol{F_A}$ and $\boldsymbol{F_B}$ bands) for all compounds.
- Non polar solvent and Polar aprotic solvents, increase intensity of $\boldsymbol{F_A}$ band was observed.
- Time Dependant Fluorescence at ***nano second*** does not show the signal for fluorescence decay confirms the *pico second* fluorescence decay can reveal the correct information about decay, presently under investigation.
- As per our understanding Dual fluorescence behavior is observed due to rotation of -SCN moiety.
- In direct proof for our hypotheses is confirmed by the single crystal XRD of **4-Thiocyanato aniline salts** (compound **5** and **6**) and their single fluorescence spectra.
- In present set of compounds, TICT Mechanism and charge separation both are playing the important role for Dual Fluorescence although our conclusions is based on liquid state fluorescence study.

## 7.12 References


[1] E. Lippert, W. Lüder, F. Moll, W. Nägele, H. Boos, H. Prigge, I. Seibold-Blankenstein, *Angew. Chem.* **1961**, *73*, 695-706; (b) E. Lippert, W. Luder, H. Boos, A. Mangini, *Editor A. Mangini, Pergamon Press: Oxford* **1962**, p443.

[2] G. Köhler, P. Wolschann, K. Rotkiewicz, in *Proc. Indian Acad. Sci.-Chem. Sci., Vol. 104*, Springer, **1992**, pp. 197-207.

[3] (a) O. S. Khalil, R. Hofeldt, S. McGlynn, *Chem. Phys. Lett.* **1972**, *17*, 479-481; (b) O. S. Khalil, R. Hofeldt, S. McGlynn, *J. Lumin.* **1973**, *6*, 229-244; (c) O. S. Khalil, R. Hofeldt, S. McGlynn, *Spectrosc. Lett.* **1973**, *6*, 147-165; (d) J. Meeks, J. Arnett, D. Larson, S. McGlynn, *Chem. Phys. Lett.* **1975**, *30*, 190-194.

[4] E. M. Kosower, H. Dodiuk, *J. Am. Chem. Soc.* **1976**, *98*, 924-929.

[5] (a) E. Chandross, H. Thomas, *Chem. Phys. Lett.* **1971**, *9*, 397-400; (b) E. A. Chandross, *The Exciplex* **1975**, *187*.

[6] (a) K. Rotkiewicz, K. Grellmann, Z. Grabowski, *Chem. Phys. Lett.* **1973**, *19*, 315-318 (b) Z. Grabowski, K. Rotkiewicz, W. Rubaszewska, E. Kirkorkaminska, *Acta Phys. Pol. A* **1978**, *54*, 767-776.

[7] (a) K. A. Zachariasse, T. von der Haar, A. Hebecker, U. Leinhos, W. Kuhnle, *Pure Appl. Chem.* **1993**, *65*, 1745-1750 (b) W. Schuddeboom, S. A. Jonker, J. M. Warman, U. Leinhos, W. Kuehnle, K. A. Zachariasse, *J. Phys. Chem.* **1992**, *96*, 10809-10819.

[8] (a) A. L. Sobolewski, W. Domcke, *Chem. Phys. Lett.* **1996**, *250*, 428-436; (b) A. L. Sobolewski, W. Domcke, *Chem. Phys. Lett.* **1996**, *259*, 119-127; (c) A. Mordzinski, A. L. Sobolewski, D. H. Levy, *J. Phys. Chem. A* **1997**, *101*, 8221-8226.

[9] K. Zachariasse, M. Grobys, T. Von der Haar, A. Hebecker, Y. V. Il'ichev, O. Morawski, I. Rückert, W. Kühnle, *J. Photochem. Photobiol., A: Chem.* **1997**, *105*, 373-383.

[10] (a) P. M. Woods, C. Kouveliotou, E. Göğüş, M. H. Finger, J. Swank, C. B. Markwardt, K. Hurley, M. van der Klis, *Astrophys. J.* **2002**, *576*, 381; (b) H. Bischof, W. Baumann, N. Detzer, K. Rotkiewicz, *Chem. Phys. Lett.* **1985**, *116*, 180-185.

[11] (a) Z. R. Grabowski, K. Rotkiewicz, A. Siemiarczuk, *J. Lumin.* **1979**, *18*, 420-424; (b) G. Z R, *Nouv. J. Chim* **1979**, *3*, 443.

[12] P. Taylor, P. Ghalsasi, P. Lahti, *Tet. letters* **2004**, *45*, 6295-6298.

[13] C. Rullière, Z. R. Grabowski, J. Dobkowski, *Chem. Phys. Lett.* **1987**, *137*, 408-413.

[14] J. A. Mondal, M. Sarkar, A. Samanta, H. N. Ghosh, D. K. Palit, *J. Phys. Chem. A* **2007**, *111*, 6122-6126.

[15] A. Bangher, R. Guy, Y. Pichot, J. Sillence, C. Steel, F. Swinbourne, K. Tamiatti, *Spectrochim. Acta Part A: Molecular and Biomolecular Spectroscopy* **1995**, *51*, 1703-1713.

[16] (a) P. Bhattacharyya, S. Bera, *Phys. Chem. Chem. Phys.* **1999**, *1*, 3253-3258; (b) S. Dähne, W. Freyer, K. Teuchner, J. Dobkowski, Z. Grabowski, *J. Lumin.* **1980**, *22*, 37-49; (c) J. Dobkowski, E. Kirkor-Kamińska, J. Koput, A. Siemiarczuk, *J. Lumin.* **1982**, *27*, 339-355.